HARVESTING ELECTRICAL ENERGY FROM MECHANICAL VIBRATION BY PIEZOELECTRIC MATERIALS AND PERFORMANCE OPTIMIZATION

A THESIS SUBMITTED TO
THE BOARD OF GRADUATE PROGRAMS
OF
MIDDLE EAST TECHNICAL UNIVERSITY, NORTHERN CYPRUS CAMPUS

BY

FESTUS OLUSOJI, OGUNJINMI

IN PARTIAL FULFILMENT OF THE REQUIREMENTS
FOR
THE DEGREE OF MASTER OF SCIENCE
IN ELECTRICAL AND ELECTRONICS ENGINEERING

SEPTEMBER 2022

Approval of the Board of Graduate Programs

Prof. Dr. Cumali Sabah
Chairperson

I certify that this thesis satisfies all the requirements as a thesis for the degree of Master of Science

Prof. Dr. Murat Fahrioğlu
Program Coordinator

This is to certify that we have read this thesis and that in our opinion it is fully adequate, in scope and quality, as a thesis for the degree of Master of Science.

Prof. Dr. Murat Fahrioğlu
Supervisor

Examining Committee Members

Prof. Dr. Murat Fahrioğlu	METU NCC/EEE	
Asst. Prof. Dr. Çanras Batunlu	METU NCC/EEE	
Assoc. Prof. Dr. Davut Solyalı	EMU/EEE	

I hereby declare that all information in this document has been obtained and presented in accordance with academic rules and ethical conduct. I also declare that, as required by these rules and conduct, I have fully cited and referenced all materials and results that are not original to this work.

Name, Last Name: Festus Olusoji, Ogunjinmi

Signature:

ABSTRACT

HARVESTING ELECTRICAL ENERGY FROM MECHANICAL VIBRATION BY PIEZOELECTRIC MATERIALS AND OUTPUT VOLTAGE LEVEL OPTIMIZATION

Ogunjinmi, Festus Olusoji
Master of Science, Electrical and Electronics Engineering
Supervisor: Prof. Dr. Murat Fahrioğlu

September 2022, 66 pages

The energy conversion performance of piezoelectric cantilever-beam energy harvesters (PCEH) is improved by developing and designing a novel. A rectangular hole is located in the middle of the metal substrate. Using the mathematical model of the PCEH, the mathematical expression of the following is derived as the eigenfrequency, displacement of the proof mass, and output voltage and power level achieved due to displacement of the cantilever carrying the piezoelectric material. We analyze the eigenfrequency and frequency domain of the model using NANOHUB to investigate the effects of frequency, load resistance, and acceleration on voltage and power. To further optimize the energy conversion of the piezoelectric using cantilever and boost converter an experimental verification was conducted. A novel PCEH has an optimal peak output power of 3451.55 µW and 5121 mV, at 0.01v diode voltage threshold of a rectifier circuit while the converter boost output yielded 15V from 5121 mV, which is 5 V input. Due to these advantages, the novel PCEH produces the output voltage and power at a higher level and a low frequency, as well as improved energy conversion efficiency.

Keywords: Energy-conversion, Efficiency, Piezoelectric Cantilever-beam Energy harvesters (PCEH), Mathematical modelling.

ÖZ

PIEZOELEKTRİK MALZEMELERLE MEKANİK TİTREŞİMDEN ELEKTRİK ENERJİSİ ELDE EDİLMESİ VE ÇIKIŞ GERİLİM SEVİYESİNİN OPTİMİZE EDİLMESİ

Ogunjinmi Festus Olusoji
Yüksek Lisans, Elektrik ve Elektronik Mühendisliği Programı
Tez Yöneticisi: Prof. Dr. Murat Fahrioğlu

Eylül 2022, 66 sayfa

Piezoelektrik konsol-ışın enerji biçerdöverlerinin (PCEH) enerji dönüşüm performansı, bir roman geliştirilerek ve tasarlanarak iyileştirilir. Metal substratın ortasında dikdörtgen bir delik bulunur. PCEH'nin matematiksel modelini kullanarak, aşağıdakilerin matematiksel ifadesi, piezoelektrik malzemeyi taşıyan konsol yer değiştirmesi nedeniyle elde edilen özfrekans, kanıt kütlesinin yer değiştirmesi ve çıkış voltajı ve güç seviyesi olarak türetilir. Frekans, yük direnci ve hızlanmanın voltaj ve güç üzerindeki etkilerini araştırmak için NANOHUB kullanarak modelin özfrekans ve frekans alanını analiz ediyoruz. Piezoelektrikliğin enerji dönüşümünü konsol kullanarak daha da optimize etmek ve dönüştürücüyü artırmak için deneysel bir doğrulama yapıldı. Yeni bir PCEH, bir doğrultucu devresinin 0.01v diyot voltaj eşiğinde 3451.55 μW ve 5121 mV'luk optimum bir tepe çıkış gücüne sahipken, dönüştürücü takviye çıkışı 5121 mV'den 15V'a kadar 5 V giriş sağladı. Bu avantajlardan dolayı, yeni PCEH, çıkış voltajını ve gücünü daha yüksek bir seviyede ve düşük bir frekansta ve ayrıca gelişmiş enerji dönüşüm verimliliğinde üretir.

Anahtar Kelimeler: Enerji dönüşüm verimliliği, Piezoelektrik Konsol-ışın Enerji biçerdöverleri (PCEH), Matematiksel modelleme.

ACKNOWLEDGMENTS

I dedicate my master's degree qualification award and the completion of this thesis to the Glory of Almighty God from whose Grace I am alive to talk about the completion of this work, also appreciate God Almighty for the opportunity given to me to achieve this far and for the grace to complete the thesis and other related research associated with this work.

I also dedicate this to my wife Omowunmi Ogunjinmi and my children whom God has given as gifts of life to me and as well appreciate them for mutual understanding over the course of my study master's degree program.

I also dedicate this to my special Academic advisor Prof. Dr. Murat Fahrioglu whose care and mentorship cannot be quantified and as well equally grateful to Asst. Prof. Dr. Canras Batunlu from the Electrical Electronics Engineering department for knowledge-impacting support and a bit of advice toward the success of this work.

I also would like to appreciate Prof. Dr. Murat Fahrioglu for his uncommon support, effort, supervision, and guidance as sacrificial work to the success and completion of this work.

I am also grateful to Chima Daniel Nwaokete, Middle East Technical University. Sustainable Environment and Energy Systems Department. For his supports on the success of this work.

TABLE OF CONTENTS

ABSTRACT........vi

ÖZ........vii

ACKNOWLEDGMENTS........viii

TABLE OF CONTENTS........ix

LIST OF TABLES........xi

LIST OF FIGURES........xii

LIST OF ABBREVIATIONS........xv

CHAPTERS

1. INTRODUCTION........1

1.1 Historical Picture of Piezoelectric Materials........3

1.2. Piezoelectric Crystalline Structure and the term Piezoelectric........4

1.2.1 The Term Poling........6

1.2.2 Piezoelectric Material and Its Market Review Chat........7

1.3. Objectives and Limitations of this study........8

1.3.1 Thesis goal........8

1.3.2. Limitation of this thesis........9

1.3.3. Hypothesis set to achieve the study........9

2. LITERATURE REVIEW........11

2.1. Energy Transition Diagram of BC-PEH........13

3. CANTILEVER BEAM FOR PIEZOELECTRICITY........16

3.1. Detailed description of a cantilever beam for piezoelectricity........16

3.1.1. Geometry Structure of the BC-PEH........17

4. MODELING OF PIEZOELECTRIC MATERIALS.........21

4.1 Mechanical and mathematical Modeling of Piezoelectric energy harvester.........21

4.1.1 Second-order spring-mass mechanical modeling of PEH........21

4.1.2 Demonstration of mechanical strain on PZT and its equivalent electrical circuit........23

5. TYPES OF MATERIALS AND SIMULATION WORKS........26

5.1 Geometry analysis of PZT........26

5.1.1 Mechanical property analysis of PZT........26

5.1.2 Material database analysis of PZT 26
5.1.3 Simulation results 27
5.1.4 Simulation of the varied thesis generated parameter/data 30
5.1.5 Simulation of the varied thesis generated data and discussion 30
6 DISCUSSION 55
6.1.1 Cost Analysis of PZT 56
6.1.2 Proposed Engineering and Scientific Solution of PEH 57
6.1.3 Observations 58
7 CONCLUSION 60
8 REFERENCES 61

LIST OF TABLES

TABLES

Table 5.1. Geometry structure of a piezoelectric material 26

Table 5.2. Mechanical structure of PZT energy harvesting method 26

Table 5.3. Material database.. 26

Table 5.4. Thesis data for simulation work category A 32

Table 5.5. Thesis data for simulation work category B................................... 33

Table 5.6. Simulation result of serial number 1 34

Table 5.7. Simulation data of serial number 2... 37

Table 5.8. Simulation data of serial number 3... 39

Table 5.9. Simulation data of serial number 4... 42

Table 5.10. Simulation data of serial number 5... 45

Table 5.11. Simulation data of serial number 6... 47

Table 5.12. Simulation data of serial number 7... 50

Table 5.13. Thesis data for simulation work category B................................. 52

Table 6.1. Cost analysis of piezoelectric materials 57

LIST OF FIGURES

FIGURES

Figure 1.1 Demonstration of PZT operational principle 3

Figure 1.2 Crystalline structure of PZT materials 5

Figure 1.3 Poling orientation of PZT 7

Figure 1.4 Piezoelectric material and its market review chat.......................... 7

Figure 2.1 Schematic diagram of PHEH 13

Figure 3.1. Schematic diagram of BC-PEH 16

Figure 3.2. Series and parallel arrangement/connection of PZT 18

Figure 4.1. Second-order spring-mass of PZT 21

Figure 4.2. Demonstration of mechanical strain on PZT and its electrical equivalent circuit 23

Figure 4.3. Demonstration of mechanical strain on PZT 23

Figure 4.4. Demonstration of bending process of PZT 23

Figure 5.1. Displacement waveform of simulation result of default data on nano-hub tool.. 27

Figure 5.2. Frequency response function waveform of simulation result of the default data on NANO-HUB tool... 28

Figure 5.3. Input acceleration waveform of simulation result of default data on nano-hub tool.. 28

Figure 5.4. Mechanical stress waveform of simulation result of the default-data on nano-hub tool 29

Figure 5.5. Output FFT waveform of simulation result of the default data on nano-hub tool.. 29

Figure 5.6. Displacement waveform of simulation result of the default data on nano-hub tool.. 31

Figure 5.7. Applied mechanical stress waveform of simulation result of the default data on nano-hub tool 31

Figure 5.8. Input acceleration waveform of simulation result of the default data on nano-hub tool 32

Figure 5.9. Peak output power waveform of PZT of thesis experiment........ 34

Figure 5.10. Output voltage level waveform of thesis experiment 35
Figure 5.11. Displacement waveform of thesis simulation experiment 35
Figure 5.12. Applied mechanical waveform of thesis simulation experiment36
Figure 5.13. Peak output power waveform of thesis simulation experiment 37
Figure 5.14. Output voltage level waveform of thesis simulation experiment38
Figure 5.15. Displacement waveform of thesis simulation experiment 38
Figure 5.16. Applied stress waveform on PZT of thesis simulation experiment
.... 39
Figure 5.17. Peak power output waveform of thesis simulation experiment 40
Figure 5.18. Output voltage level waveform of thesis simulation experiment40
Figure 5.19. Max. displacement waveform of thesis simulation experiment 41
Figure 5.20. Applied stress waveform of thesis simulation experiment 41
Figure 5.21. Peak output power waveform of thesis simulation experiment 42
Figure 5.22. Output voltage level waveform of thesis simulation experiment43
Figure 5.23. Max Displacement waveform of thesis simulation experiment 43
Figure 5.24. Applied stress waveform of thesis simulation experiment 44
Figure 5.25. Peak output power waveform of thesis simulation experiment 45
Figure 5.26. Output voltage level waveform of thesis simulation experiment46
Figure 5.27. Max Displacement waveform of thesis simulation experiment 46
Figure 5.28. Applied stress waveform of thesis simulation experiment 47
Figure 5.29. Peak output power waveform of thesis simulation experiment 48
Figure 5.30. Output voltage level waveform of thesis simulation experiment48
Figure 5.31. Max Displacement waveform of thesis simulation experiment 49
Figure 5.32. Applied stress waveform of thesis simulation experiment 49
Figure 5.33. Peak output power waveform of thesis simulation experiment450
Figure 5.34. Output voltage level waveform of thesis simulation experiment51
Figure 5.35. Max Displacement waveform of thesis simulation experiment 51
Figure 5.36. Applied stress waveform of thesis simulation experiment 52
Figure 5.37. Peak output power waveform of thesis simulation experiment 53
Figure 5.38. Peak voltage level waveform of thesis simulation experiment. 53
Figure 5.39. Max Displacement waveform of thesis simulation experiment 54
Figure 5.40. Applied stress waveform of thesis simulation experiment 54

Figure 6.1. Schematic diagram of BC-PEH and DC-DC converter 55
Figure 6.2. PLECS online simulation result of BC-PEH and DC-DC converter
.... 56

LIST OF ABBREVIATIONS

ABBREVIATIONS

T	Temperature
Tc	Currie temperature
BC-PEH	Cantilever Beam-Piezoelectric Energy Harvester
PEH	Piezoelectric Energy Harvester
EMEH	Electromagnet Energy Harvester
B	Magnetic flux density
S	Area of the coil
PZT	Piezoelectric transducer

CHAPTER 1

INTRODUCTION

Mechanical waves from Sound energy and other environmental energy sources are unexplored sources of energy with exceptional ability to meet the future expanding energy requirement to play a vital role as a renewable source of energy [1]. Due to efficiency problems, this technology is currently not readily usable, but the research being conducted in the field indicates it may be useful in the future.

In addition to being environmentally friendly and cost-effective, powering circuit systems with ambient energy also breaks the limitations imposed by traditional batteries. Electronics are capable of being distributed in places where it is inaccessible to change or recharge batteries, such as deep wells or nuclear power plants. As a result of the Internet of Things (IoT), especially, future generations will also benefit, [6]

There is a wireless data exchange between a network of sensors powered by a wireless network [2]. A further advantage is that energy harvesters themselves may be used as sensors to estimate extreme values. Recently, the development and application of energy harvesting have become increasingly popular due to advancements in large-scale integration technology and low-energy-cost electronics. In addition to light, heat, electromagnetic fields, and vibrations, there are other types of environmental energy, the benefit of harvesting energy from mechanical vibrations lies in the fact that they are ubiquitous and can be harvested regardless of the season [9]. Weather, and location. With vibrational energy harvesters having relatively high energy densities (0.37 watts/mm^3) and low-power circuits and sensors available (µW - mW range) [4], [6].

Vibrational energy harvesting could be applicable in a wide range of applications of Piezoelectric energy harvesting material is attaining an interesting point in engineering specialization and technological base where power requirements for electronics devices have been reduced as well as increasing the potential of its application in energy conversion technology.

Among all energy harvester technologies, piezoelectric material with its vibration characteristics has been identified with unique features and emerged as a method of choice power as an alternative energy source for operating micro-scale devices. Piezoelectric materials' potential for application can be maximized to handle a wide range of input frequencies and compression giving rise to energy harvesting to exist.

Referencing the law of conversation of energy which states that "energy cannot be created nor be destroyed", The form of mechanical energy created by sound waves can be converted into other forms, such as heat energy or electric energy, with a suitable and reasonable approach.

The recovered output power of a piezoelectric which will be extensively discussed in this thesis can instantly be applied to power microelectronics devices like Bluetooth, GPS modules, microcontrollers, and low-power units. However, further research in my future work will deliver a more usable and highly improved power output for purpose of serving as an alternating power supply and possibly reducing energy demand with the ability to be enlisted among other renewable energy systems.

Further to the discussion of the promising potential of piezoelectric material, among other methods of energy harvesting methods which will be briefly stated in this paper, this thesis will focus on piezoelectric material energy harvester as a more reliable harvesting method of mechanical vibration into electrical energy due to the unique features, high energy density and high-efficiency factor. A good sizeable piezoelectric material that can convert up to 80% of mechanical energy to electricity.

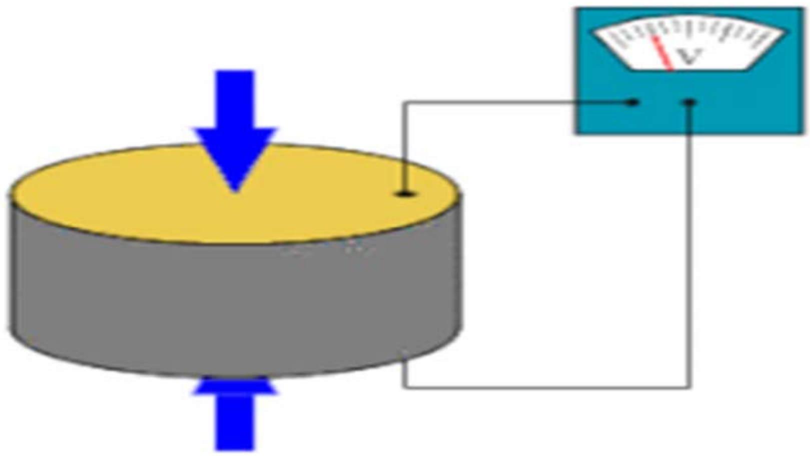

Experimental demonstration of the principle of operation of piezoelectricity from piezoelectric material

Figure1.1 Demonstration of PZT operational principle

1.1 Historical Picture of Piezoelectric Materials

Piezoelectricity was first discovered in 1980 by two brothers and French scientists Jacques and Pierre Curie, [11] While experimenting with a variety of crystals they discovered that applying mechanical pressure to specific crystal-like quartz released an electrical charge and this is what is referred to as piezoelectricity. During world war1, piezoelectricity was used for practical application in sonar. Sonar works by connecting a voltage across a sonar transmitter but the focus of this research is direct piezoelectricity which is a piezo-generator that converts the applied mechanical pressure to equivalent electrical energy. Piezoelectricity is a phenomenon that describes the coupling between the electrical and mechanical states of the material. When a piece of piezoelectric material is mechanically displaced or deformed by a wave, and thereby exists trading back and forth of kinetic energy and potential energy on the plate which constitutes an electric charge of the atomic particle with an equivalent voltage on the plate. This is referred to as piezoelectricity.

1.2. Piezoelectric Crystalline Structure and the term Piezoelectric

Piezo is coined from the Greek word which means ‘rush’ or ‘‘squash’. Piezoelectricity is a property of certain dielectric materials to physically deform in the presence of an electric field, or conversely, to produce an electrical charge when mechanically deformed. There are a wide variety of materials that exhibit this phenomenon to some degree, including natural quartz crystals, semi-crystalline polyvinylidene polymer, polycrystalline piezoceramic, bone, and even wood. Piezoelectricity is due to the spontaneous separation of charge with certain crystal structures under the right conditions. This phenomenon, referred to as spontaneous polarization, is caused by a displacement of the electron clouds relative to their atomic centers, i.e. a displacement of the positive ions relative to the negative ions within their crystal cells. Such a situation produces an electric dipole However, the electric field effect between the charged particle determine the strength of the piezoelectricity effect and this is a measure of the term POLING. If the dipole exists in random motion, then the polarization of the dipole becomes weak and the piezoelectricity becomes low, this is a normal state of a piezoelectric material.

Pierre Curie and Jacques Curie published their first experimental demonstration of piezoelectricity in 1880. Using crystals of tourmaline, quartz, topaz, cane sugar, and Rochelle salt, they predicted crystals' behavior by combining their knowledge of pyroelectricity and the underlying crystal structures that lead to pyroelectricity. By applying mechanical stress to these crystals, such as pressure or vibration, the Curie brothers discovered that electricity generated, which is proportional to the applied stress. Furthermore, they observed that the crystalline orientation of their chosen materials, along with the piezoelectric properties of the materials, was crucial to creating the conditions for electricity to be generated from mechanical application. It wasn't until Langevin and French co-workers perfected an ultrasonic submarine detector during World War I that piezoelectric devices were used in a serious manner. Piezoelectric ceramics were developed in the second world war by the United States, Japan, and the Soviet Union. Energy harvesters, sensors, and actuators.

In addition, the Piezoelectric effect exists in two domains; namely, the direct piezoelectric effect and the indirect piezoelectric effect. The direct piezoelectric effect describes the ability to convert mechanical energy to electrical energy which is also known as the generator or transducer effect while the converse piezoelectric effect describes the ability to transform electrical energy to mechanical energy which is also known as the motor/actuator effect. The electrical energy generated by the direct piezoelectric effect can be stored to power electronic devices and it is known as "energy/power harvesting".

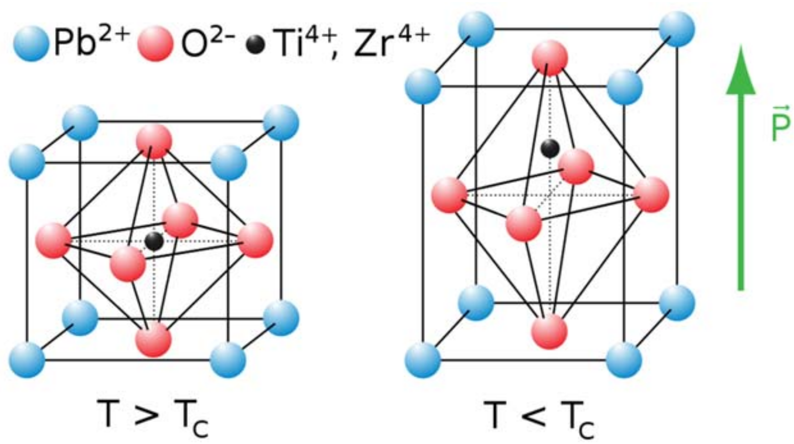

Figure 1.2. crystalline structure [16]

The PZT is formed from lead zirconate-titanate and generates more output voltage effect than quartz under the same measured vibration.

The default orientation of rotation or movement of a dipole of crystals of piezoelectric material is random naturally. When PZT is compressed, the polarization of dipole occurs due to atomic crystalline structure, consequently, an electric charge is generated in the material. However, these charges exist in dipole that vibrates and are set into the rotational motion which invariably moves in a direction that reduces the net electrical and mechanical energy stored in the dipoles. If the rotation orientation of the dipoles is random, then the net polarization of the crystal dipole will yield no significant change, hence the strength of the piezoelectricity is weak or negligible.

This is what determines the piezoelectricity effect and as well dictates the power output of the piezoelectric materials in general. The figure below describes the scenario of the negligible piezoelectricity effect.

However, this orientation of rotation of the dipole is technically referred to as poling. Poling is referred to as the direction of aligning the dipole of the crystalline structure of a piezoelectric material. Therefore, poling is a prime determinant of the strength of piezoelectricity of a PZT material. This is an intrinsic piezoelectric effect in lead-zirconate, where the charged zirconium or titanium ions move relative to the center position of the crystallite above and below the Curie temperature TC. Piezoelectric materials possess crystalline structures in which the center of positive and negative charges does not overlap, yielding dipole moments. The term dipole moments describe the measurement of the separation between the positive and the negative charges within a given or common system. Therefore, when piezoelectric crystals undergo stress as a result of push or pull, then PZT crystal experiences the polarization of dipoles, creating electrical charges. Tension and compression generated voltages of opposite polarity, and in proportion to the applied force, [8]

1.2.1 The Term Poling

From Figure 1.2a. shown below describes the default orientation of motion of dipole of a piezoelectric material crystalline structure and its negligible resulting power output performance due to cancellation of electric charges and decrease in the electric field intensity as much as the resulting potential difference between the output terminal.

Where Figure 1.2b. as shown below replicates the poling process of the dipole with the orientation of the dipoles in the same direction, hence creating more and strong field intensity thereby exerting a force to move the adjacent same charged-particles in the same direction, with an increase in the net potential across its terminal increases significantly. Consequently, the piezoelectricity in this context of poling is quite higher and stronger than the scenario of Fig 1.2a. since there is no cancellation of charges and the intensity of the electric field increases with poling. Hence the stored electrical charges increase significantly and the output power performance is said to be magnificently high concerning to poling effect.

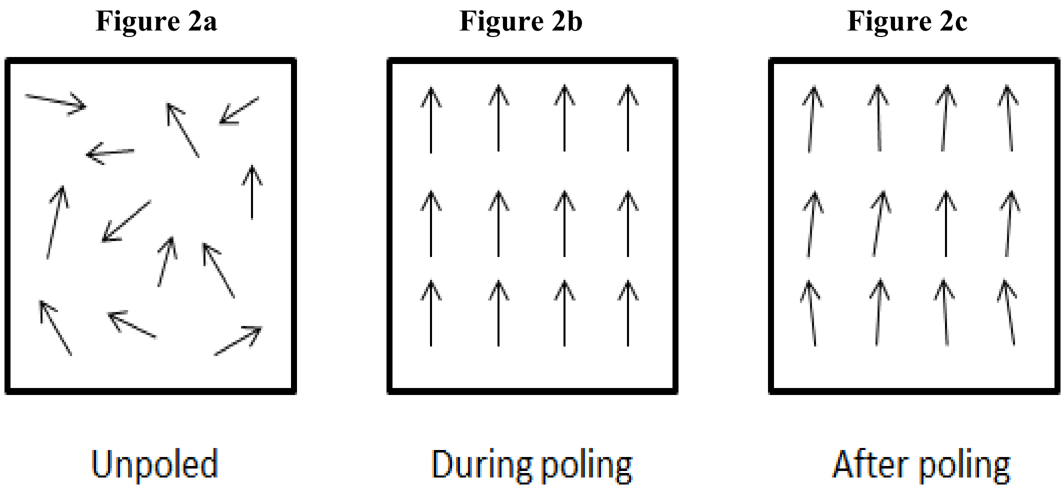

Fig 1.3. Poling Orientation of PZT Crystals [16]

1.2.2 Piezoelectric Material and Its Market Review Chat

As shown in the figure below, depicts market review of piezoelectric materials corresponding to their applications and market share (%) IN 2007. Piezoelectric material is one of the most widely used according to the usage trend over time, because of their wide bandwidth, fast electromechanical response, relative low power requirement, high energy density and, high generative forces.

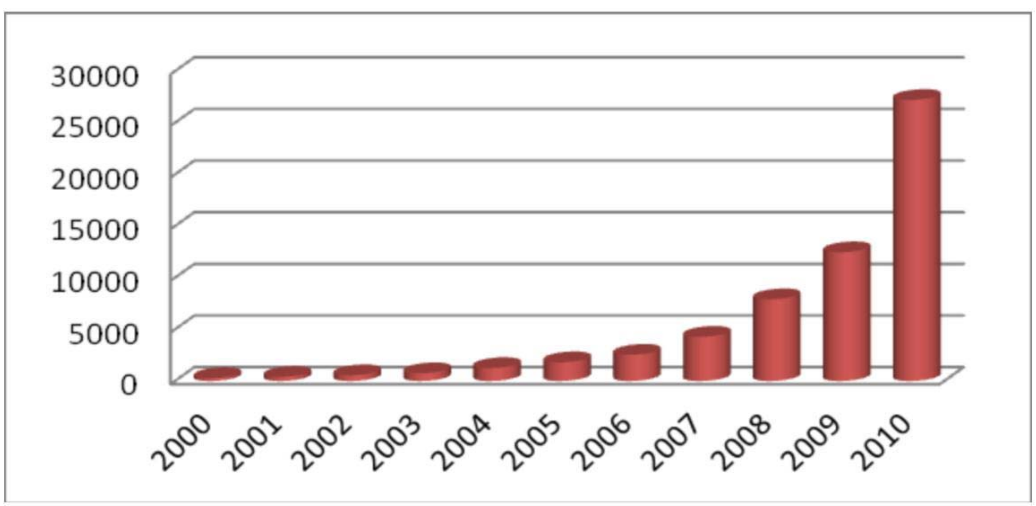

Fig 1.4. Piezoelectric Material Market Review Chat

1.3. Objectives and Limitations of this study

1.3.1 Thesis Goal

The primary objective of this thesis work is to improve the performance of PZT in terms of the peak power and output voltage level of cantilever-based piezoelectric energy harvesters such that the proposed and improved output performance can solve a scientific and engineering problem identified in the EV industry. The major problem associated with a long range of an EV is attributed to the specific state of charge of cells of a battery pack in an electric vehicle such as hybrid electric vehicles (HEV), Plugin-hybrid electric vehicles, (PHEV), and extended range electric vehicle(E-REV).

This state of charge of a battery pack determines the total energy that can be delivered to the vehicle engine to sustain the movement of an electric vehicle. However, this total energy to be delivered from the battery back is limited due to self-discharge and cell imbalance conditions. The application of this proposed solution emanating from the improved power and output voltage level of a cantilever-based PZT can be applied to compensate for cells' self-discharge and potentially increases the cell energy level. In addition, this application will enhance the EV range and as well improve its efficiency and performance.

1.3.2. Limitation of this thesis

Due to the high-power application requirement to cause a drift of electrons of a high number of cells from their cathode electrodes to the anode electrodes and generate electric charges. Therefore, improved PCEH cannot be used to charge a high capacity battery of an EV battery pack or drained/deeply discharged high capacity battery because of the high current requirement to restore charges of such battery and as well to fast charge the battery, However, it is advantageous in floating the battery voltage such as Nickel-cadmium battery and lead acid battery only or in any system of technology where energy storage devices are used for grid support grid back up such as uninterrupted power supply. since float charging or trickle charging is not required in lithium-ion battery technology. Since this technology cannot meet up with the high current requirement for such high-power applications of charging deeply discharged batteries or high-capacity batteries, then the range of its application is limited by this factor.

1.3.3. Hypothesis set to achieve the study

It is hypothesized that resonant frequency is a key factor in achieving the maximum output peak power and voltage level. So, the cantilever substrate is carefully selected of a brass alloy and the thickness of the PZT and cantilever are varied accordingly to derive the highest possible output voltage level and peak output power.
The maximum output voltage and peak power are obtained when the thickness of the PZT and Cantilever substrate assumes equal or almost equal with increasing the mass of the body attached at its free end. there is the flexibility of obtaining a higher output voltage by increasing the thickness of the substrate and PZT along with the mass of the body and this makes this study or technology feasible,

In addition, the output voltage can be further stepped up with a dc-dc converter to increase the level of the output voltage depending on the desired output level requirement.

The mass of a body hung by the free end of the cantilever is as well carefully varied such that the excitation frequency of the PZT is almost equal or equal to the resonant frequency of the system to achieve a better output performance.

Temperature of the system affects the output performance and this is adequately considered to avert an unusual increase in the system temperature above the specified limit called Curie temperature.

CHAPTER 2

LITERATURE REVIEW

Zhou et al. (2014) reviewed the piezoelectric energy harvester for the possibility of replacing batteries in the future and to realize the independent power supply of wireless sensor nodes [1]. An ad hoc network of wireless sensors is generally composed of several low-cost low-power microsensors spread over a particular area, collecting, and processing the pertinent information and then transferring it cooperatively to a base station by means of wireless communication.

Nowadays, batteries are utilized to provide energy for wireless systems that are intended to last for years or decades in most cases. As a result of the limited size of the node, battery energy cannot satisfy the requirements because it is very limited [12]. Power supply has therefore become a major problem of network system development and application because it limits the lifetime of sensor nodes

Chen et al. (2015) investigated an integrated energy harvester with PZT and electromagnet mechanism for wireless sensor application in a smart grid [2]. Wireless sensor nodes in smart grids can be powered by hybrid energy harvesters combining piezoelectric and electromagnetic mechanisms [4], [5]. Printed circuit boards (PCBs) are surrounded by induction coils in the proposed energy harvester device, which uses permanent magnets attached to cantilevers. Piezoelectric cantilever arrays are excited by the magnetic field of charging conductors carrying alternating currents (ACs). Piezoelectric and electromagnetic transduction mechanisms convert vibration energy into electric energy. Fabrication and testing of a prototype measuring 50*50*12 mm^3 were performed. The proposed energy harvester can generate up to 295.3 μW when it is connected to a conductor that carries 2.5 A at 50 Hz, and 46.6 μW when its piezoelectric elements are combined with electromagnetic elements.

Therefore, having carefully compared the two-test conducted, according to Chen et al. the result shows that the total output power of 341.9 μW obtained, the power density is much greater than the one output result of normal BC-PEH under the same condition. Xiong et al. (2020) researched on improvement work of energy performance of BC-PEH, [3]. The development and design of a novel piezoelectric cantilever-beam energy harvester (BC-PEH) are made to improve the energy conversion performance of the typical BC-PEH. A rectangular hole is drilled through the middle layer of the metal substrate. Mathematical expressions are derived for the eigenfrequency, displacement of the attached mass, and output voltage and power of the PCEH from the mathematical expression. A study of frequency, load resistance, and acceleration on voltage and power was performed using COMSOL and MATLAB to verify the validity of the model. Conclusively, experiments were conducted to further verify the results. Using the novel BC-PEH, the appropriate output power is 10.69 mW, and the first-order eigenfrequency is 43.7 Hz. Consequently, the neoteric BC-PEH converts energy more efficiently as it has a lower frequency, a broader frequency band, and a higher output voltage and power.

Some studies proposed and examined a hybridization scheme with electromagnetic induction to improve the power density of the piezoelectric energy harvester [3], [4]. To increase piezoelectric energy harvester (PEH) power density, an innovative hybridization scheme that utilizes electromagnetic transduction. By replacing the mass block by a magnet array and adding a coil array, we created the hybrid energy harvester (BC-PEH) based on the basic cantilever piezoelectric energy harvester (BC-PEH). An alternating magnet array was used in the electromagnetic energy harvester to increase its output power.

Output power experiments was performed and conducted as a means of comparing the power density of the hybrid harvester and BC-PEH. Using 18.6 Hz and 0.3 g, the hybrid harvester and BC-PEH had power density values of 3.53 mW/cm^3 and 5.14 $\mu W/cm^3$, respectively. Hence, the hybrid harvester has a power density 686 times greater than the BC-PEH, proving that EMEH hybridization can improve power density. In addition, the hybrid harvester is capable of charging 2.2 mF capacitors within 17 seconds, which is better than previous models. The development of self-powered devices is a vital step towards a sustainable society.

Shan et al. (2015) investigated the power output improvement of hybrid energy harvester [5]. An equation for calculating the output power of a piezoelectric-electromagnetic hybrid energy harvester (PHEH), incorporating the secondary piezoelectric effect. As a result of the revamped/improved external load, the hybrid energy harvester could achieve a 13.3% higher system power output than with a single piezoelectric generator. It is also found that damping parameter matching helps the hybrid energy harvester achieve a 23% increase in peak output, Experimental verification of the numerical model was performed using hybrid energy harvesting [3], [4], [5].

2.1. Energy Transition Diagram of BC-PEH

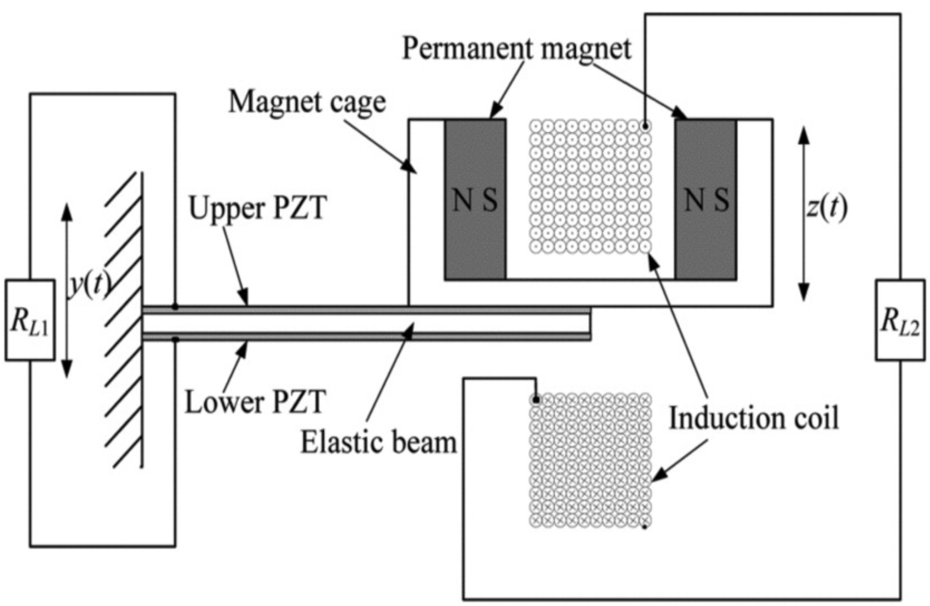

Fig 2.1. Schematic diagram of PHEH [17]

There are also studies that reviewed the analytical mode of wire-band low frequency PEH for extracting the maximum ambient vibration [1], [6]. Microelectronic systems have been enhanced by advancements in fabrication technology and integration levels, sensor networks and the Internet of Things have developed as a result of the growth of small structures and microsystems, so that a substantial number of industries, housing, healthcare, and other services are now fully digitized, automated, and linked.

A microsystem with a very low power requirement ranging from microwatt to milliwatt. However, does not require frequent maintenance and battery refurbishment

Naano et al. (2019) reviewed piezoelectric energy harvester device for low-frequency range (0-100 Hz) with a developed application to improve the power output of piezoelectric energy harvester through the recreation of actual excitation and geometrical conditions expected on pallet lift and storage systems, the performance of the piezoelectric vibration energy harvesters was explored experimentally [7].
Shindo et al. (2003) investigated PEH polarization switching under mechanical stress [8]. The deformation responses of PZT was observed and recorded under different magnitude of applied mechanical force and the crystal polarization. PZT crystals or ceramics can fail structurally or develop dielectric breakdowns under extreme mechanical and electrical loading. PZT ceramics have undergone several tests to determine how they fracture under mechanical and electrical pressures.

Several studies show that ubiquitous low frequency vibration energy has potential to generate high output power at low frequencies, [4] [5] [9]. Asthana et al. (2020) researched on amplifying energy from broadband energy harvester and its equivalent electrical model [10]. Another research reviewed the theory of effect of piezoelectric material crystals and its discovery by Curie [11]. Anisi et al. (2017) investigated on PEH routing based and battery power-based routing approaches in wireless sensor network [12].

Some studies reviewed the bending properties of amalgamated PZT with glass fiber and equivalent electrical performance and dipole behavior, during mechanical load acting on it. [1] [6] [13]. Piezoelectric composite thin plates are analyzed analytically for bending properties as a function of bending temperature. Incorporating glass fiber resulted in nearly four times more bending strength and approximately two times more Young's modulus in the length direction.

The bending properties and output voltage performance of composite PZT has also been investigated [1] [13] [14].

This was approached by combining CFRP electrodes with epoxy resin containing potassium sodium-niobate piezoelectric nanoparticles, this composite sample could be successfully polarized [1] [13] [14]. In addition, the bending behavior of the samples was compared using a three-point bending method. According to the simulation, the peak output voltage produced by 98.4 MPa of bending stress was 0.51 mV. We also found that 0.01546% was obtained for its efficiency after the transformation.

Furthermore, Dhote et al. (2016) in their study found that Low-power sensor nodes can be powered by piezoelectric vibration energy harvesters. Broad bandwidth is one of the main requirements for energy harvesters. This requirement cannot be met by a conventional linear harvester. This leads to a shift in research focus toward utilizing non-homogeneity to extend the harvester's bandwidth. The reverse sweep exhibits a reduced response compared to the forward sweep, despite nonlinear techniques being promising for extending a bandwidth. [15]

CHAPTER 3

CANTILEVER BEAM FOR PIEZOELECTRICITY

3.1. Detailed description of a cantilever beam for piezoelectricity

A cantilever is a deigned structural element that extends horizontally with two different points A and B. where A is a pivoted end and the other end B is made free. However, a load can be attached for any intended purposes. The structural load could be regarded as any material or object that has the potential to exert a weight or pressure on the beam when applied horizontally to the beam, hence, it is a force, deformation, or acceleration applied to structural elements

piezoelectric cantilever beam can be structurally arranged or assembled such that the beam material and two piezoelectric material strips, conductive adhesive substance, and two piezoelectric films by series or parallel arrangements, At the extreme of a cantilever there is a block that can enhance the vibration amplitude of cantilever beam as well as changing the frequency of its vibration according to the Figure shown below

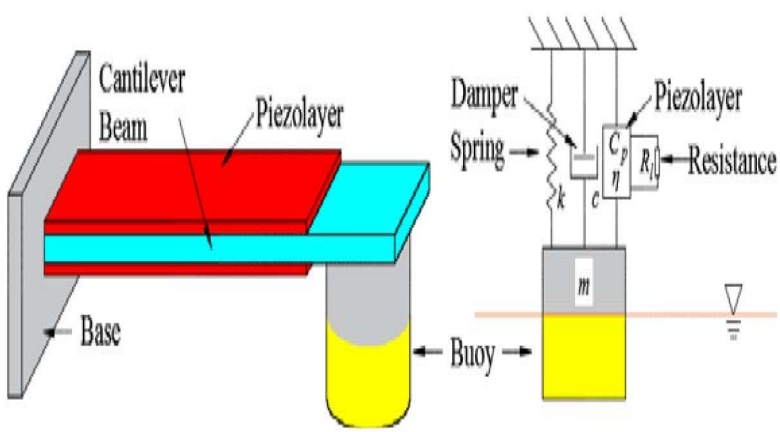

Fig 3.1. Schematic diagram of BC-PEH

3.1.1. Geometry Structure of the BC-PEH

In this thesis work, the table below shows the materials and dimensioning of the materials used for this simulation, hence they are categorized into different structures and properties.

The figures below show the structure of a typical BC-PEH, and it comprises the following

- a pivot,
- a beam,
- an attached mass of a body,

As described in Fig 3.1 shown above, a cantilever has one of its end points fixed to its base while the other end is allowed to move freely. Two layers of PZT are mounted on the beam of a cantilever at both upper layer and lower layer of the beam. A mass of a body or a load can be attached to its free end of the beam. The concept of this thesis mainly is to identify, discuss and implement the method of performance improvement of the system in terms of eigenfrequency, peak power output, and output voltage delivered by the energy harvester. The performance output quantity of the energy harvester depends on the geometry structure of the energy harvester system which determines the following parametric functions.

- Eigenfrequency
- Coupling mode
- Input acceleration due to mass of the body
- Thickness of PZT-5H
- Type of materials
- Length of a cantilever beam
- Nature of substrate material used.

3.1.2. Infrastructural Method of design configuration

The method of design configuration of piezoelectric-cantilever energy harvester, in this thesis, involves extensively, the method of connection of energy harvester.

Cantilever-Piezoelectric energy harvester has two distinct slabs known as the upper slab of the piezoelectric and the lower slab of piezoelectric, these two overlays are mounted on the beams with a separating substrate metal of brass material as used in this work. When a mass of a body is attached at the free end of the cantilever, there exist extensions and compressions. When the two layers of the energy harvester are poled in opposite directions, this type of connection is called series connection or series arrangement of the system as shown in figure 4a below. Alternatively, when they are connected or arranged in such a way that the energy harvesters' poles are in the same direction, in this case, it is called a parallel connection or parallel arrangement of the system as depicted in figure 4b below. However, parallel connection/arrangement of piezoelectric energy harvester is used in this thesis.

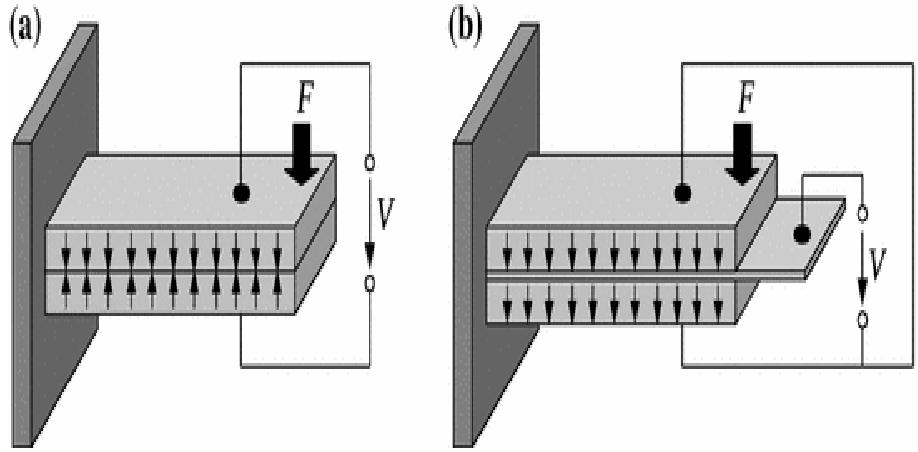

3.2 Series and parallel arrangement/connection of PZT

The separation of the metal substrate allows a capacitance to exist between the piezoelectric materials and invariably determines the magnitude of the output voltage and current of the system. The capacitance between two parallel plates is directionally proportional to the smallest area of the plates and inversely proportional to the distance between the plates From the Figure 3.1a. shown above, during the mechanical vibration leading to an oscillatory motion, two major damping forces exist in the system acting toward the equilibrium state of the body.

These are the mechanical damping force due to friction and the resistance offered due to air, which is known as air resistance. Therefore, the total damping forces existing in the system can be generally shown as d.

The movement of the mass at the free end of the cantilever as represented in its model exert a mechanical pressure and causes it to extend and compress which is generally referred to as deformation of the PZT, due to this deformation of the energy harvester(transducer), In addition, the applied mechanical pressure is equivalently converted to electrical energy and measurement taken with the aid of voltmeter.

However, the transducer creates and exerts a damping/restoring force $\mathbf{F_e}$ on the body causing a mechanical pressure/displacement and vibration of the transducer, and this momentarily reduces the forces of the transducer as well as the deformation.

As a result of the interconnection of the electrical interface circuit, [10] the electrical damping force is generated $\mathbf{d_e}$ which is represented as γe.

In analysis, PZT uses a couple of methods which is referred to as constitutive equation as shown below. Hence, this is called a constitutive equation

$$S = S^E \cdot \underline{T} + d^t \cdot \underset{\sim}{E} \text{ ---------------- equation (1)}$$

$$\underline{D} = d \cdot \underline{T} + \varepsilon^T \cdot \underset{\sim}{E} \text{ ---------------- equation (2)}$$

$$C = \varepsilon \frac{A^2}{d} \text{ ---------------------- equation (4)}$$

Where ε represents the absolute permittivity of the dielectric of the energy harvester,

A is the area of the smallest of the two energy harvester layers

d is the distance separating the two layers of the plates.

In the thesis work, the mass of the body attached to the free end of the beam is a variable type, where the same object with different masses is used and different eigenvalues are observed as well as the resonant frequency is taken.

At different masses, different eigenfrequencies, resonant frequencies, output voltages, and power are measured and recorded for 20 different tests and simulations as shown in the result expressed in **table 5.4**, in **Chapter 5** as shown.

CHAPTER 4

MODELING OF PIEZOELECTRIC MATERIALS

4.1 Mechanical and mathematical Modeling of Piezoelectric energy harvester.

A second-order spring mass damper can be used as a modeling technique/strategy or mechanical kinetic traducer (PZT) as represented below in figure 8a, the figure below shows the interconnection of the attached lumped element with the energy harvester (PZT), connected with the electrical interface circuit. According to the diagram below, the transducer is represented by the mass **m.**

The mass is suspended on a string of stiffness, **Ks** creating resonance frequencies to the eigenfrequencies of the attached transducer (PZT). Beam

4.1.1 Second-order spring-mass mechanical modeling of PEH

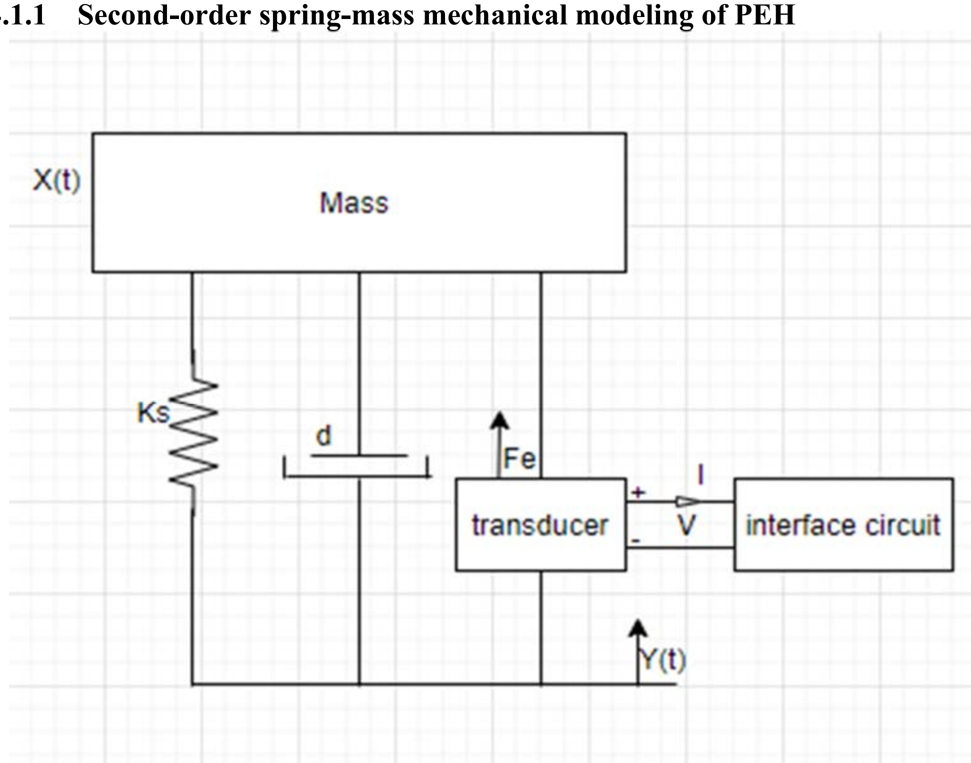

Fig 4.1. Second order Spring Mass

$$\boldsymbol{Y(t) = ysin2\pi ft}$$ **--------------------equation (5)**

$$\boldsymbol{X(t) = xsin2\pi ft + \phi}$$ **--------------equation (6)**

Where **y** represents the amplitude of motion of the transducer (Frame/PZT),

x represents the amplitude of the motion of the attached mass,

$\boldsymbol{\phi}$ represents the angular phase difference between the displacement amplitude of the PZT (**frame**) and the displacement amplitude of the attached **mass (m)** at the cantilever free end.

$$ma = mx + dx + f_e + kgx$$

$$ma = mx + (de + d)x + kgx$$ ---------equation (7)

Mechanical damping is represented by $\gamma d = \frac{d}{2m\omega_n}$

Electrical damping is represented by $\gamma e = \frac{d}{2m\omega_n}$

The natural frequency of the cantilever beam system can be represented as

$$\omega_n = \sqrt{\frac{k_s}{m}}$$ --------------- equation (8)

Let **σ** represent the sum of the mechanical damping force (γd) and the electrical damping force (γe), such that

$$\boldsymbol{\sigma} = \gamma d + \gamma e$$

$$\frac{x(s)}{y(s)} = \frac{s^2}{(s^2 + 2\boldsymbol{\sigma}\omega_n + \omega^2{}_n)}$$

The power output of the system can be expressed as

$$p = \frac{[\![(x]\!]^2 de)}{2}.$$

Such that input mechanical damping is equal to electrical damping.

4.1.2 Demonstration of mechanical strain on PZT and its electrical equivalent circuit

As a result of the interconnection of the electrical interface circuit, [10] the electrical damping force is generated d_e which is represented as γe

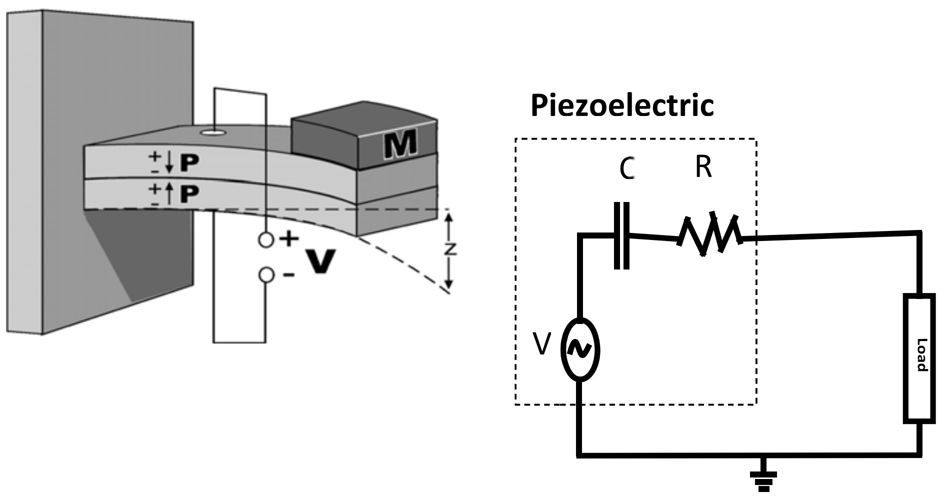

Fig 4.2. Demonstration of mechanical strain on PZT

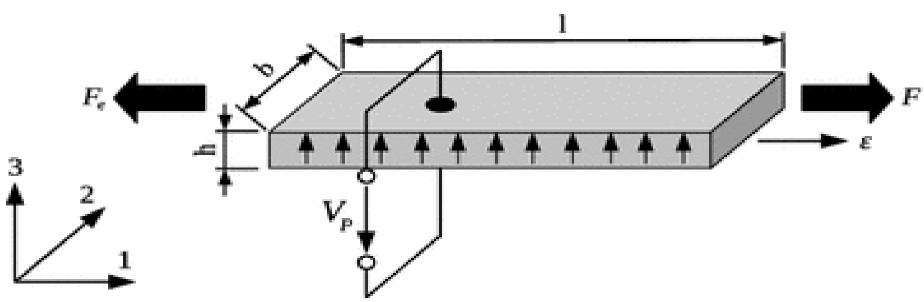

Fig 4.3. Demonstration of mechanical strain on PZT

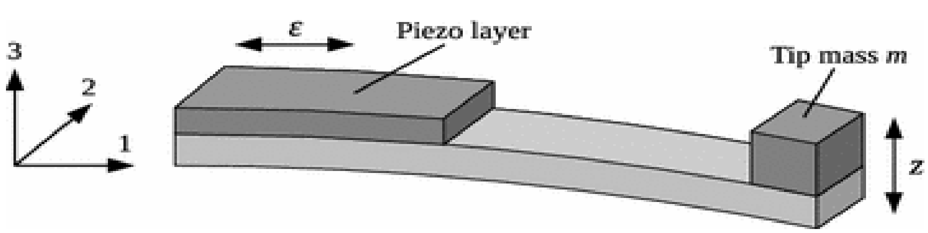

Fig 4.4. Demonstration of bending of PZT due to applied Tip mass

$$E = -\frac{v_p}{h}\ , \quad q = Dbl\ , \quad T = \frac{f}{bh} \quad , S = \frac{\varepsilon}{l} \quad , I = \frac{\partial q}{\partial t},$$

q represents the charges, F is the mechanical force acting on the PSZT due to mechanical vibration and ε is an elongation which is a resulting change in the shape of the material during compression and extension of the material when it deforms. Then the constitutive equation (1) & (2) above can be written in terms of the variables F, Ɛ, V and I, instead of S, E, D and T from the equation (1) & (2) above.

$$F = k_p \mathcal{E} + \Gamma v_p$$

$$I = \Gamma \mathcal{E} + C_p v_p$$

$$\text{Where } k_p = \frac{bh}{lS}{}_{\text{E}},\ C_p = (\mathcal{E}^{\text{T}} - \text{d}^2 / S^{\text{E}})\text{bl/h} \quad \text{and} \quad \Gamma = \frac{\text{db}_{\text{E}}}{S}$$

k_p represents the stiffness of PZT material, then piezoelectric output capacitance is denoted by C_p, and an electromechanical coupling factor is Γ. According to equation (1) shown above, a spring force is referred to as F. $k_p\varepsilon$ is material stiffness and the coupling force, and, Γv_p is determined by the voltage across the piezoelectric material. As a result of the balance of forces, F is referred to as a restoring force F_e acting on the mass as explained above. Naturally, PZT energy harvesters are extremely stiff, and this will require a good magnitude resonating frequency, provided the PZT will be suspended around the frame. Therefore, the cantilever orientation as described in figure 5 above will be considered due to large deflection in direction (3), producing a small elongation (ε) force in the direction of 1 as shown above in figure 5. Hence the constitutive equation in equations 1 and 2 described above is still valid but can be further written as shown below.

$$F_e = k_p \text{x} + \ \Gamma v_p$$

$$\text{I} = \Gamma \text{x} - C_p v_p$$

Then mathematical derivation from figure 5a above can be written as

$$ma = mx + dx + kx + \ \Gamma v_p$$

Where $K = k_p + k_s$

The final spring damper system can be mathematically represented below as

$$ma = mx + dx + kx + \Gamma v_p$$

$$\mathrm{I} = \Gamma \mathrm{x} - C_p v_p$$

CHAPTER 5

TYPES OF MATERIALS AND SIMULATION WORKS

Type of materials is another crucial practice that should not be under-estimated in this concept of technology, most especially it forms an important fundamental factor of PZT-energy harvester power output performance optimization.

5.1 Geometry analysis of PZT

Table 5.1. Geometry analysis of PZT

S/N	GEOMETRY ANALYSIS		
1	PZT-5H thickness	256µm	
2	The thickness of the substrate	140µm	
3	length of substrate	24.53mm	
4	length of the proof mass	0.05mm	
5	width of the proof mass	6.4mm	
6	Gap	24mm	
7	number of layers used	2	
8	types of connection	parallel	

5.1.1 Mechanical property analysis of PZT

Table 5.2. Mechanical property analysis of PZT

S/N	MECHANICAL PROPERTY ANALYSIS		
1	proof mass	1mg	
2	end mass density	1900kg/m^3	

5.1.2 Material database analysis of PZT

Table 5.3. Material database analysis

S/N	MATERIAL DATABASE ANALYSIS		
1	Piezoelectric	PZT-5H	
2	Substrate	Brass	

The simulated results are represented by the figures shown below. The figure 5.1 below shows the maximum and minimum displacement of the energy harvester, figure 5.2 represents the frequency response function between the cantilever and the energy harvester while figures 5.4 and 5.5, shows the stress and Fourier frequency transformation of the system.

The average power and the measured output voltages are extremely low. The simulation output performance is dependent on several functions: the resonant frequency, the mass of the attached mass of a body at the free end of the cantilever, and the acceleration of the attached body. The waveforms shown of figures 5.1, 5.2, 5.3, 5.4, 5.5, are software default setting while the thesis work simulation works are other figures as shown with their respective waveforms.

5.1.3. Simulation results

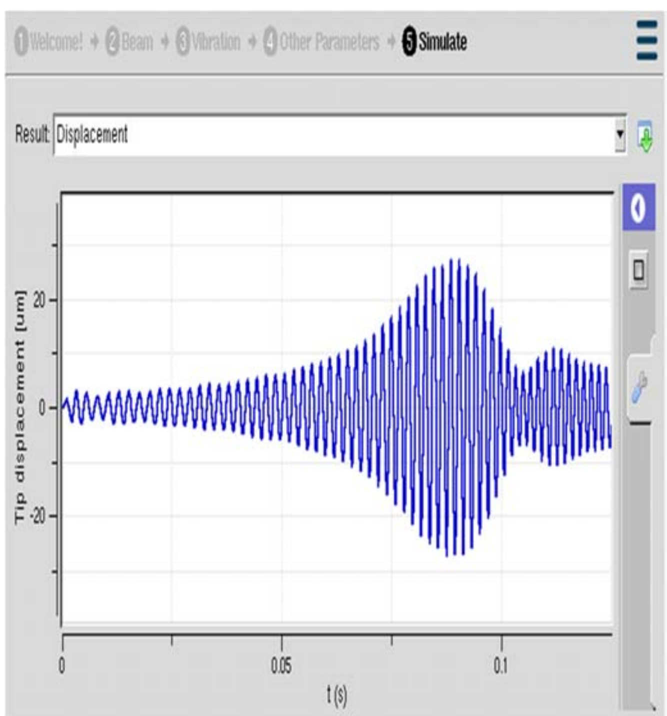

Figure 5.1. displacement waveform of simulation result

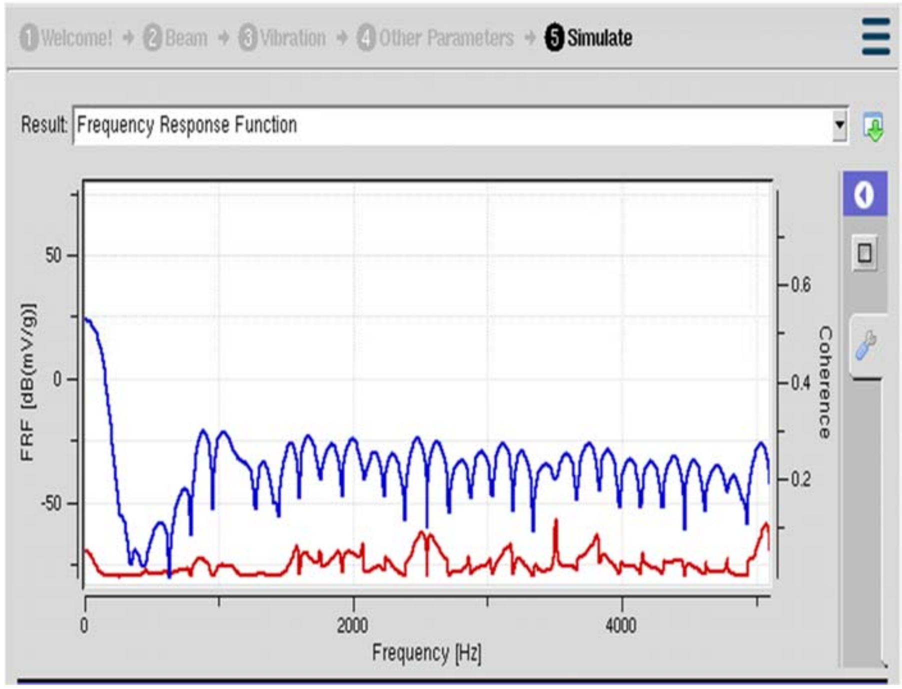

Fig 5.2. Frequency Response Function waveform of simulation result

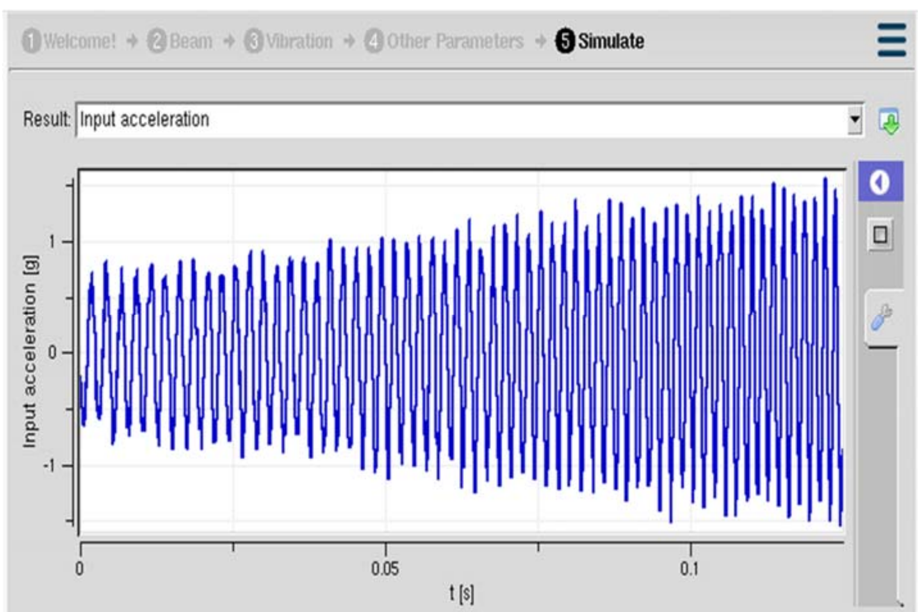

Fig 5.3 Input Acceleration waveform of simulation result

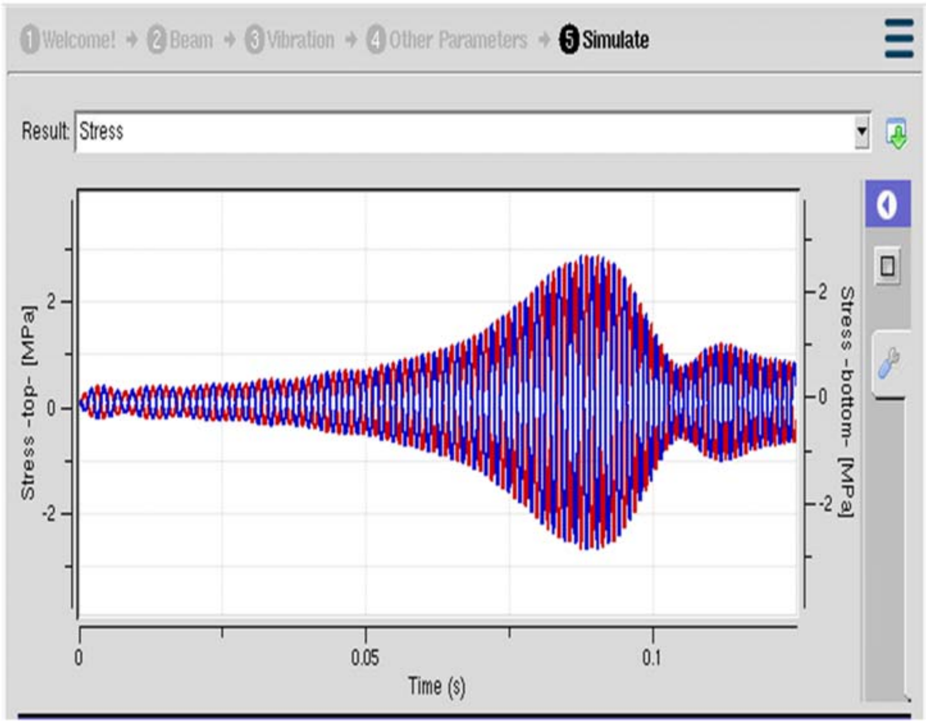

Fig 5.4. Mechanical Stress waveform of simulation result

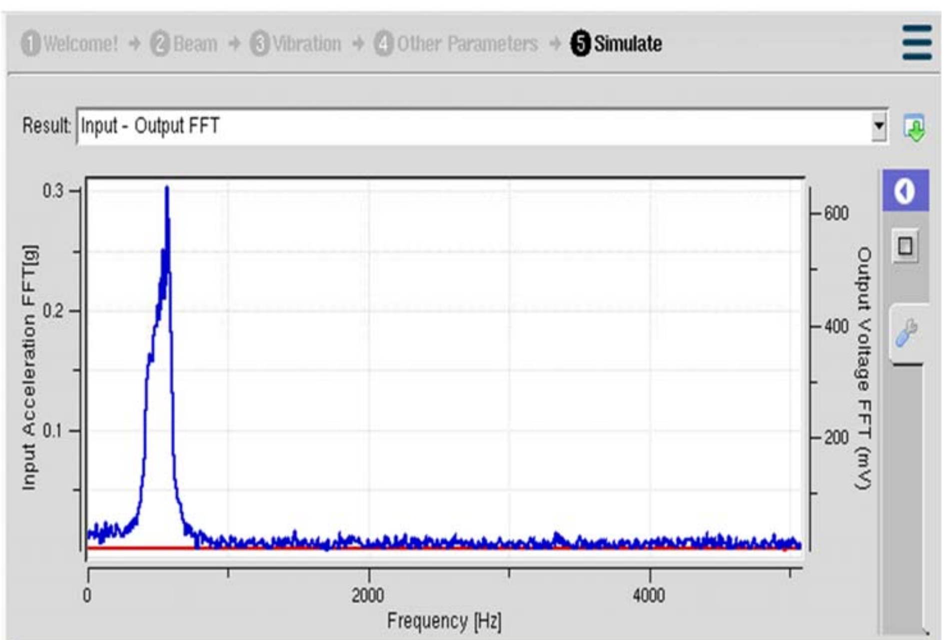

Fig 5.5. Output FFT result

5.1.4 Simulation of the varied thesis generated parameter/data

The second simulation is performed while other output performances determining factors are varied accordingly to obtain an improved performance as described below.

The frequency of the vibrating body and the cantilever is affected by the mass of the attached body which invariably determines the output power performance of the system. As the mass of the attached body increases from 1mg to 0.3 g and the end mass density decreases from 1900-kg/m^3, the output peak power performance dropped from 13.317 μW to zero with a corresponding low frequency.

From the simulation result, as the attached mass of the body increases, the stiffness of the set-up increases and consequently reduces the frequency with zero output power performance. The figures shown below are the simulated result of decreasing displacement of the energy harvester and the cantilever bean but the input displacement increases. figure 5.6, the stress in figure 5.7, and input acceleration in figure 5.8 below.

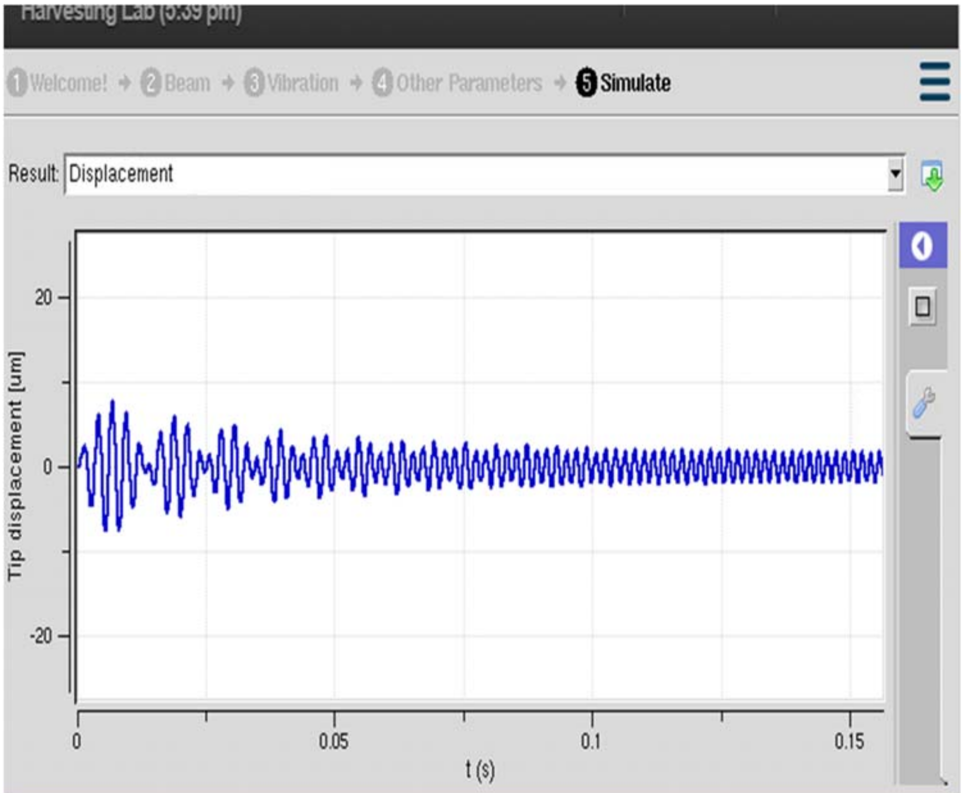

Figure 5.6. Displacement result

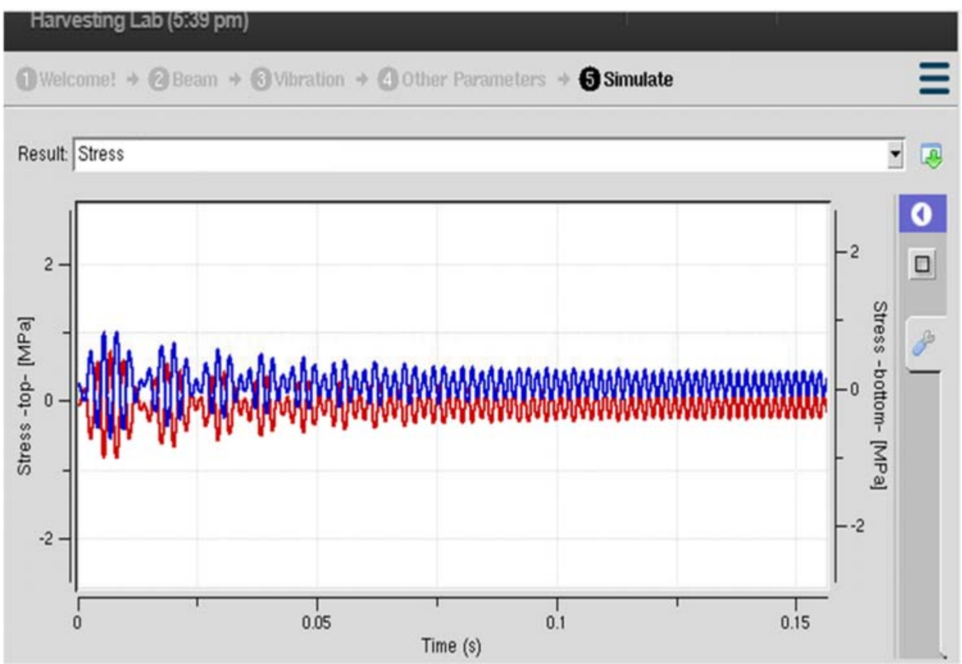

Figure 5.7. Applied mechanical stress result

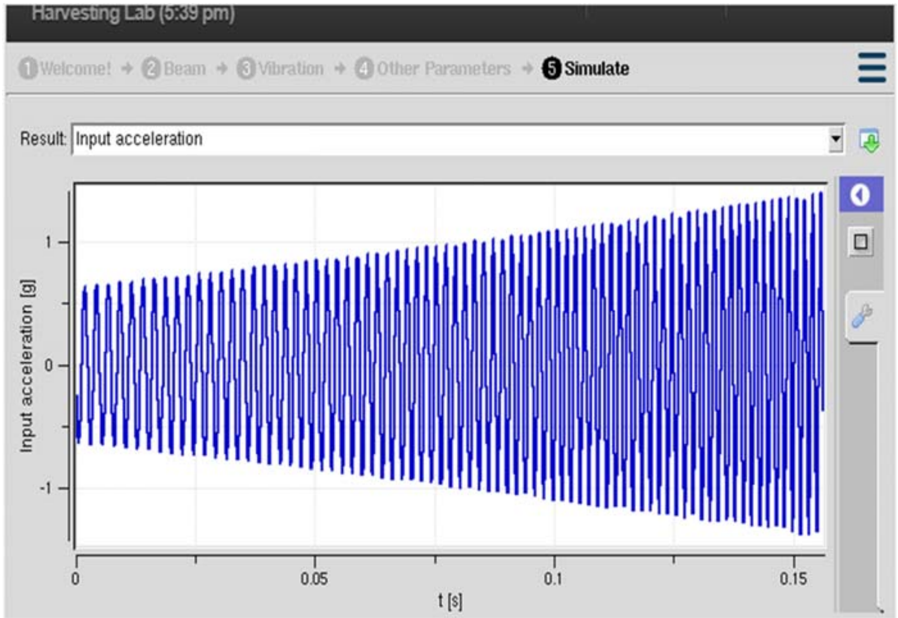

Figure 5.8. Input Acceleration result

5.1.5 Simulation results of the thesis generated data and discussion

The table below as shown describes the sequence of simulations was performed.

Table 5.4 of simulation category A.

S/N	Mass of body (g)	Thickness of PZT (μm)	Thickness of substrate (μm)	Length of substrate (mm)	Excitation/ Natural frequency Hz	Open-circuit resonant frequency (Hz)	Average harvested power (μW)	Peak power (μW)	Diode voltage Threshold	Peak Voltage (mV)
1	10	1450	1450	24.53	1118.30	1172.30	0.40	1.40	0.01	103.25
2	20	1450	1450	24.53	814.39	853.6.7	3.66	14.07	0.01	326.98
3	30	1450	1450	24.53	671.77	704.17	11.39	60.12	0.01	675.96
4	40	1450	1450	24.53	584.79	613.00	30.37	207.36	0.01	1255.35
5	50	1450	1450	24.53	524.70	550.00	45.56	597.64	0.01	1987.15
6	60	1450	1450	24.53	479.99	503.14	223.06	2246.00	0.01	4131.54
7	56.24	1450	1450	24.53	495.43	519.32	377.38	3451.55	0.01	5121.00

Table 5.5 Thesis data for simulation work category B

S/N	Mass of body (g)	Thickness of PZT (µm)	Thickness of substrate (µm)	Length of substrate (mm)	Excitation/ Natural frequency Hz	Open-circuit resonant frequency (Hz)	Average harvested power (µW)	Peak power (µW)	Diode voltage Threshold	Peak Voltage (mV)
8	60	1450	256	24.53	272.24	284.47	0.12	0.00	0.01	0.00
10	60	1450	512	24.53	306.16	320.51	0.10	1.55	0.01	14.94
11	60	1450	768	24.53	341.17	358.17	0.45	10.31	0.01	37.39
12	60	1450	1024	24.53	379.09	397.47	1.15	24.74	0.01	226.81
13	60	1450	1450	24.53	479.99	563.14	223.00	2246	0.01	4131.54

According to this works objective as clearly stated in the abstract, which is to identify, discuss, and implement a method of performance improvement of the system in terms of eigenfrequency, peak power output, and output voltage delivered by the energy harvester.

The performance output of the energy harvester is discovered to be dependent on the geometry structure of the energy harvester system which determines the following parametric functions.

- ❖ Eigenfrequency
- ❖ Input acceleration due to mass of the body
- ❖ Dimension of PZT-5H
- ❖ Nature of substrate material used
- ❖ Type of rectifier/dc-dc converter used.

Table 5.6 Simulation data of serial number 1

S/N	Mass of body (g)	Thickness of PZT (μm)	Thickness of substrate (μm)	Length of substrate (mm)	Excitation/ Natural frequency Hz	Open-circuit resonant frequency (Hz)	Average harvested power (μW)	Peak power (μW)	Diode voltage Threshold	Peak Voltage (mV)
1	10	1450	1450	24.53	1118.30	1172.30	0.40	1.40	0.01	103.25

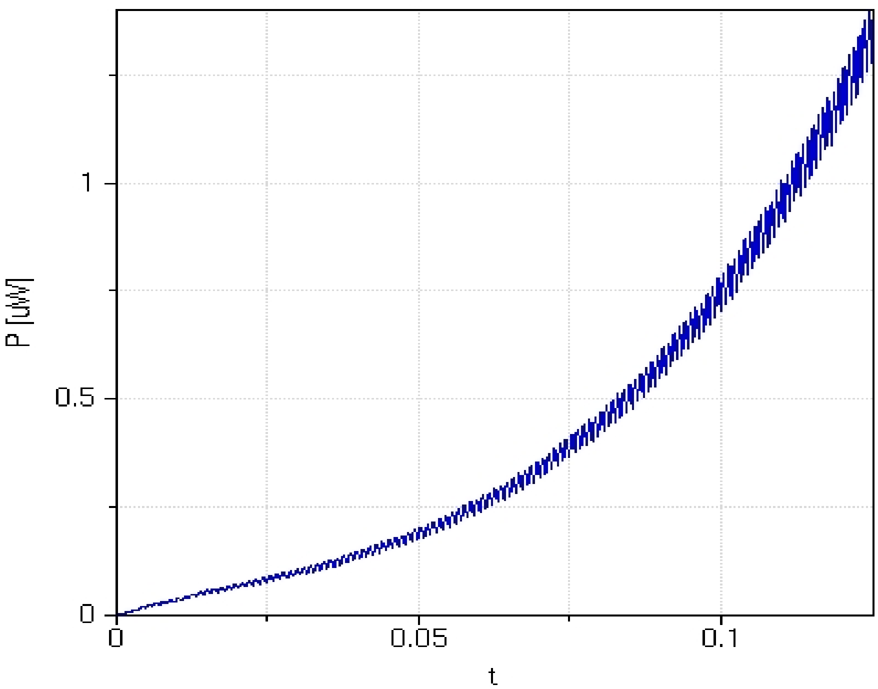

Figure 5.9. Peak Power output waveform of simulation result

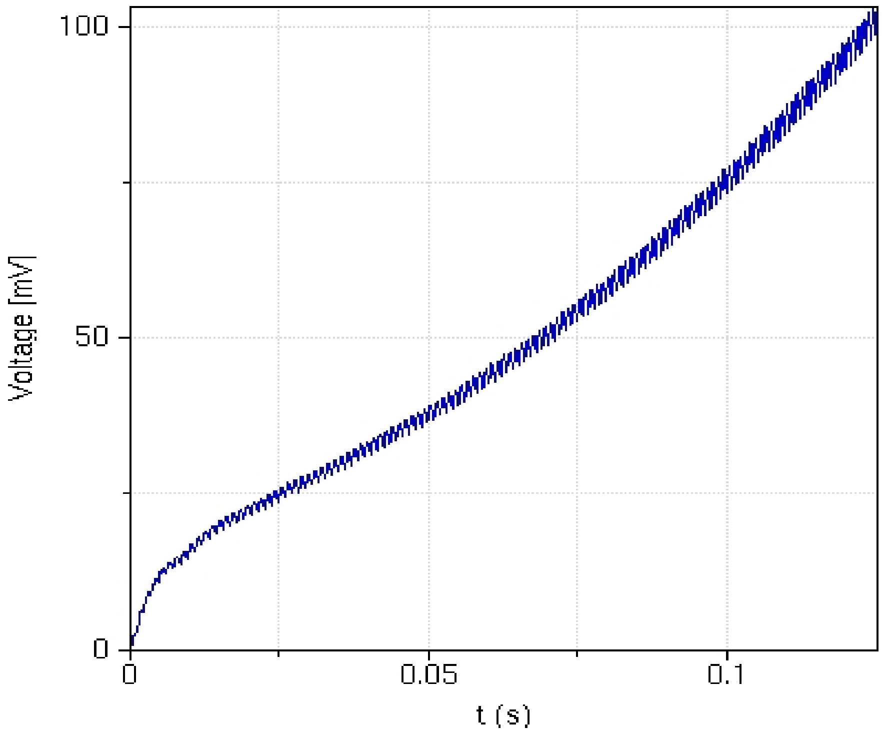

Figure 5.10. Output Voltage Level waveform of simulation result

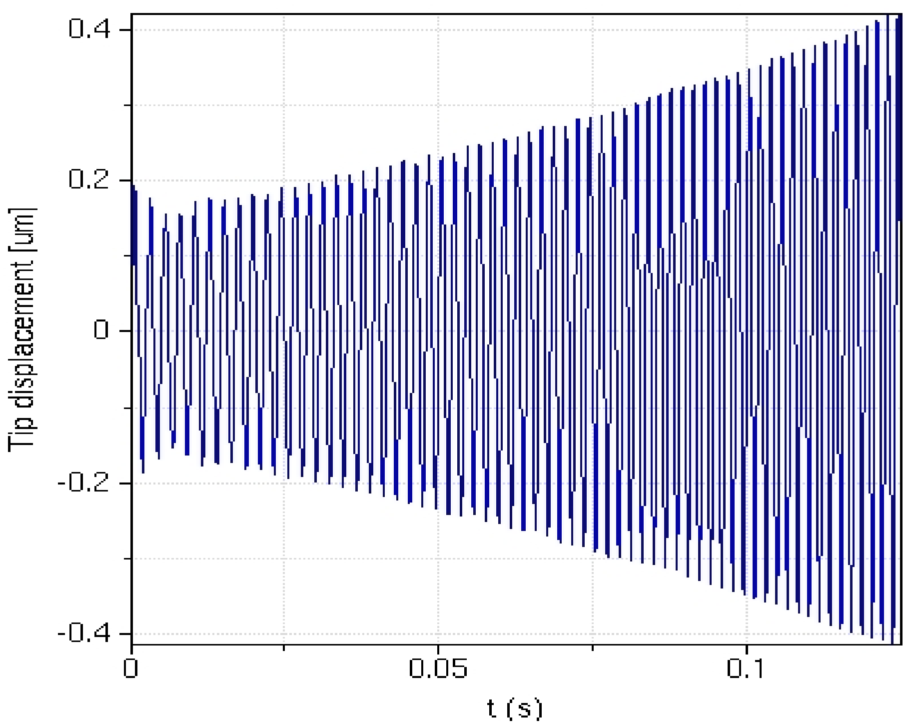

Figure 5.11. Displacement waveform of simulation result

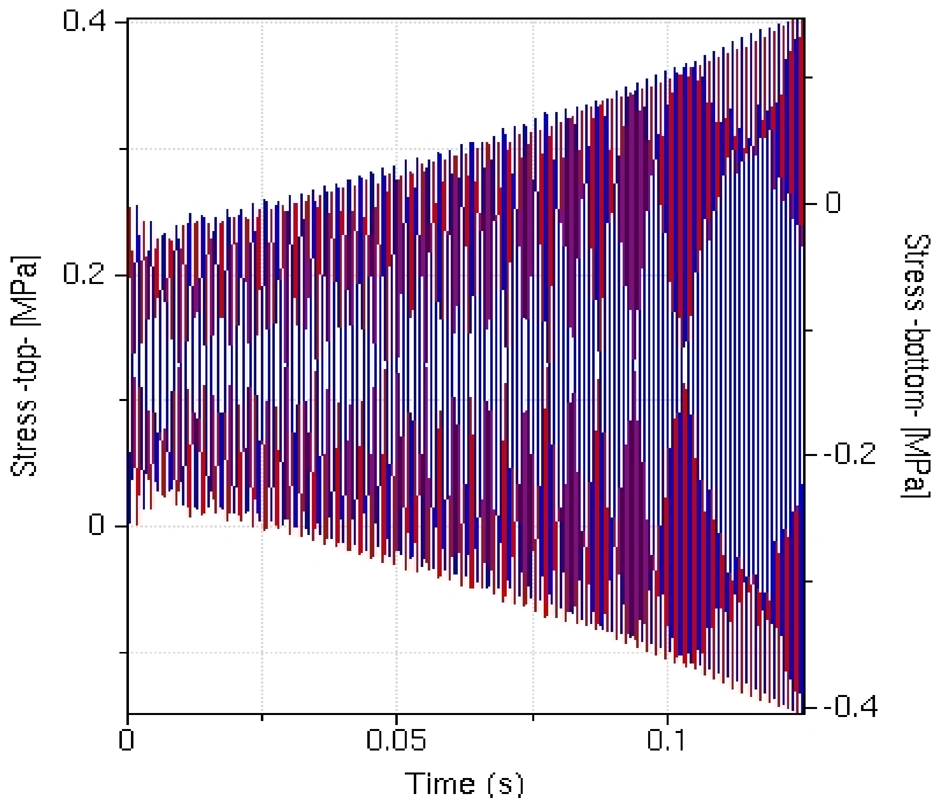

Figure 5.12. Applied Mechanical Stress waveform of simulation result

Table 5.7. Simulation data of serial number 2,

S/N	Mass of body (g)	Thickness of PZT (μm)	Thickness of substrate (μm)	Length of substrate (mm)	Excitation/ Natural frequency Hz	Open-circuit resonant frequency (Hz)	Average harvested power (μW)	Peak power (μW)	Diode voltage Threshold	Peak Voltage (mV)
2	20	1450	1450	24.53	814.39	853.6.7	3.66	14.07	0.01	326.98

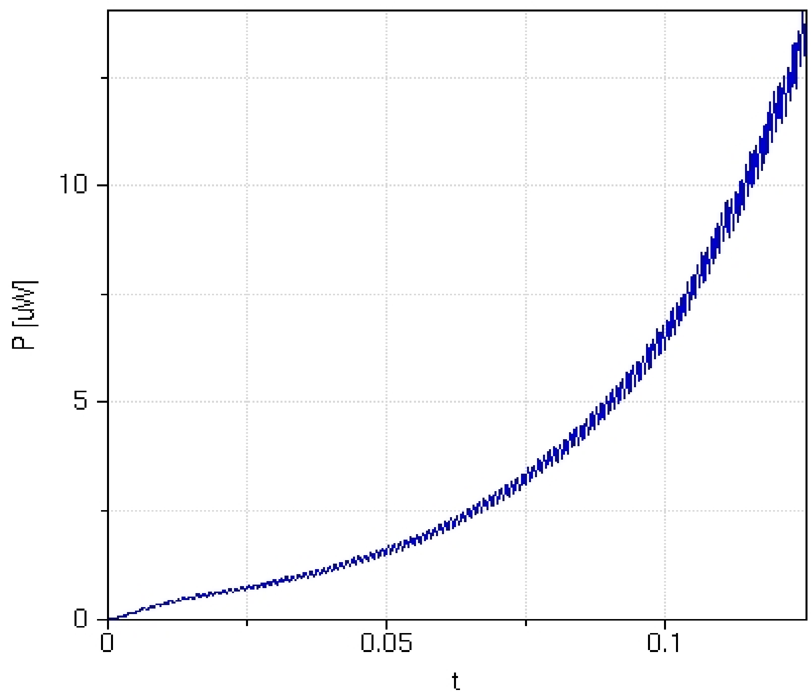

Figure 5.13. Peak power output waveform of simulation result

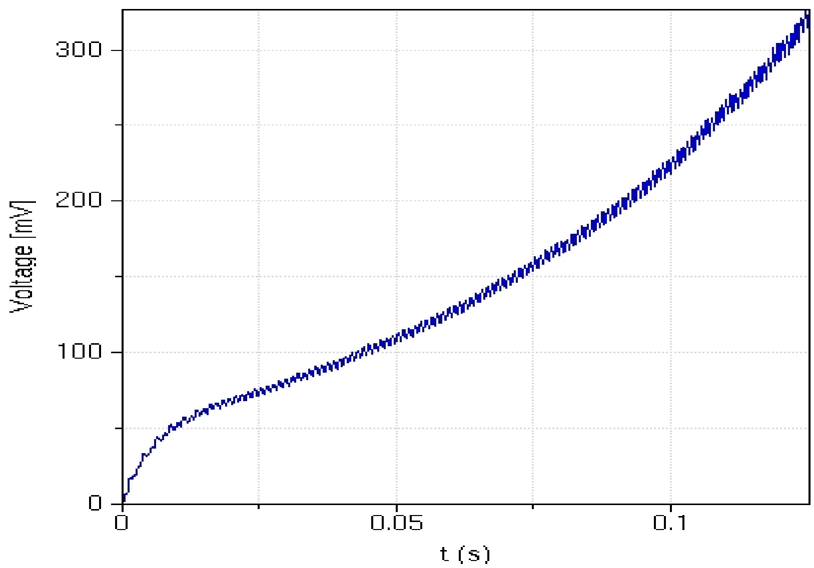

Figure 5.14. Output Voltage Level waveform of simulation result

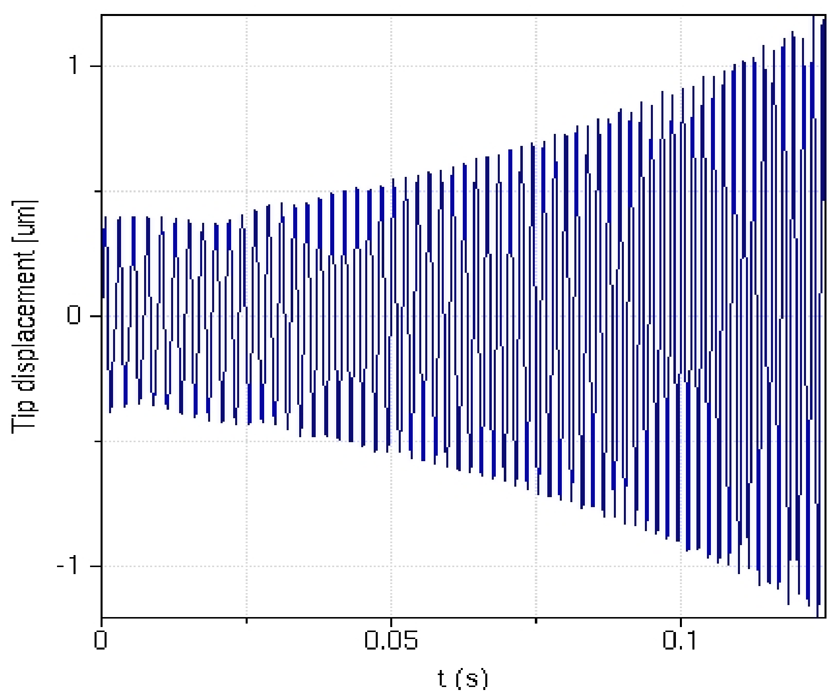

Figure 5.15. Displacement waveform of simulation result

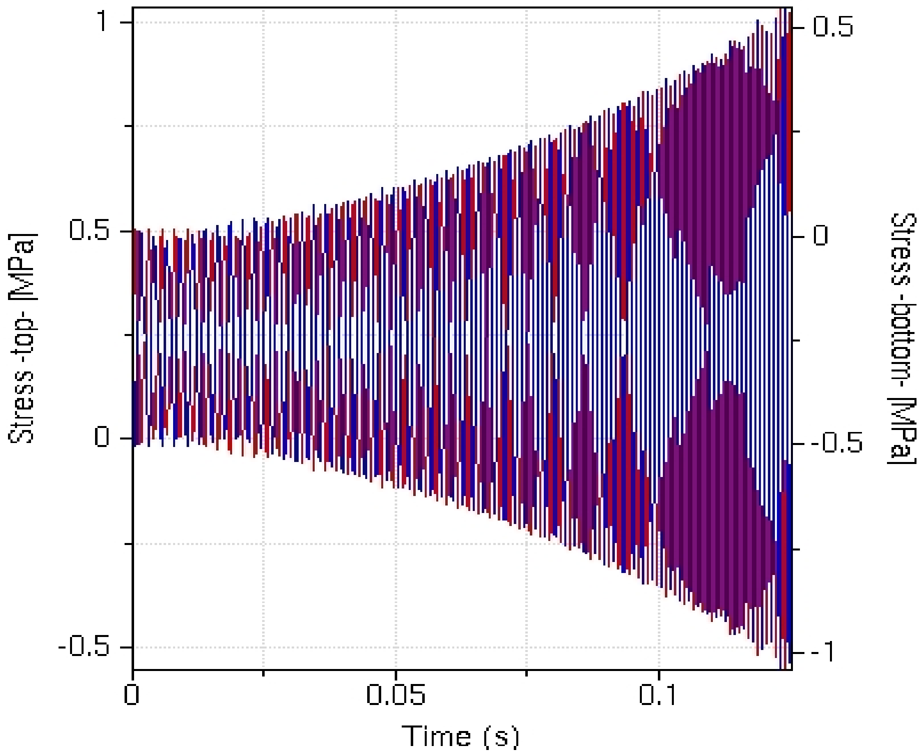

Figure 5.16. Applied Stress waveform of simulation result

Table 5.8. Simulation data of serial number 3

S/N	Mass of body (g)	Thickness of PZT (µm)	Thickness of substrate (µm)	Length of substrate (mm)	Excitation/ Natural frequency Hz	Open-circuit resonant frequency (Hz)	Average harvested power (µW)	Peak power (µW)	Diode voltage Threshold	Peak Voltage (mV)
3	30	1450	1450	24.53	671.77	704.17	11.39	60.12	0.01	675.96

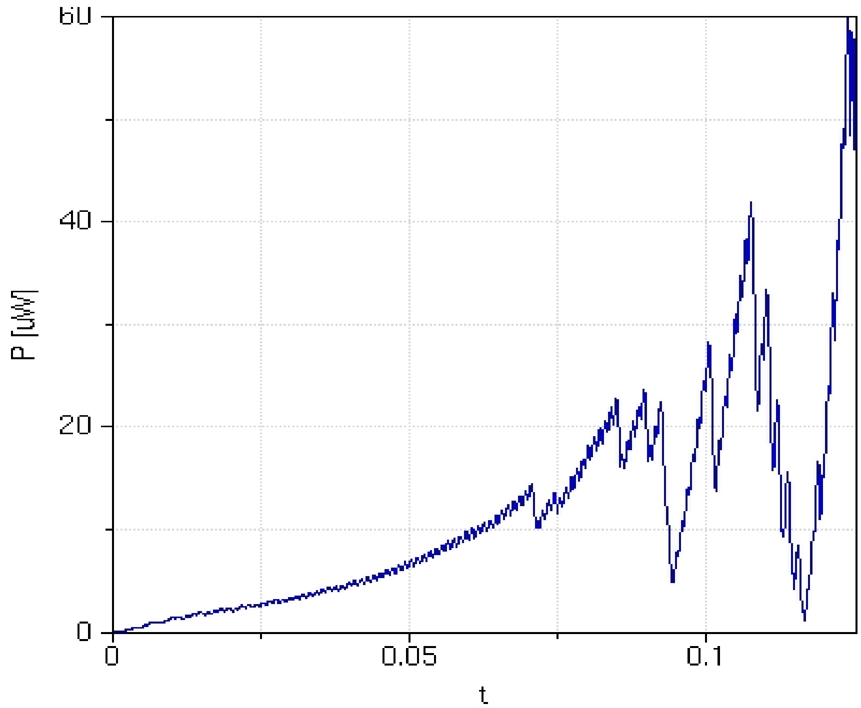

Figure 5.17. Peak Power Output waveform of simulation result

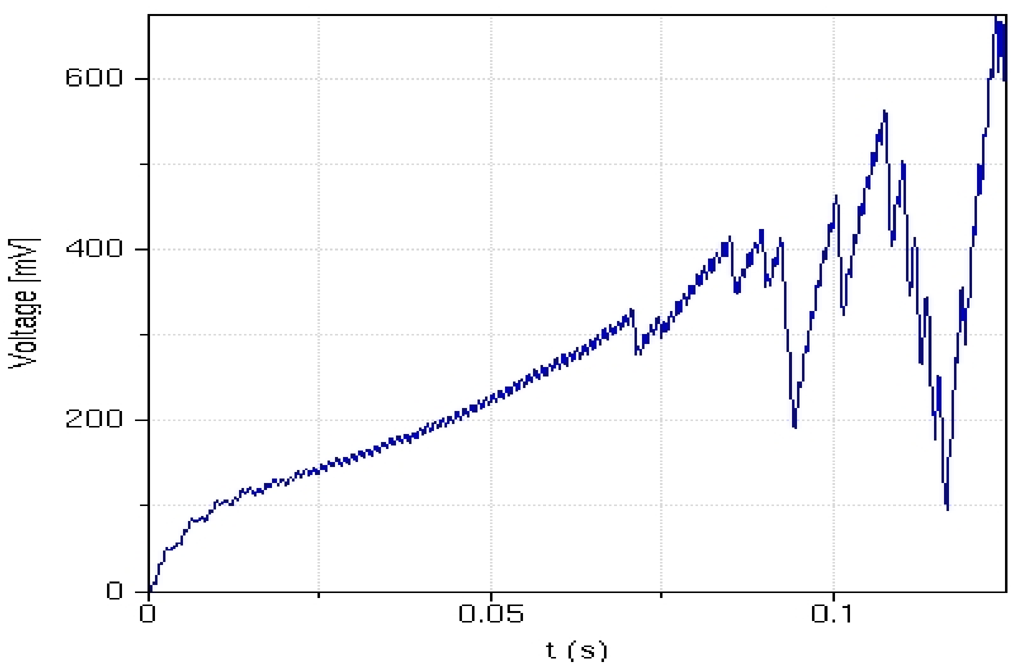

Figure 5.18. Output Voltage Level waveform of simulation result

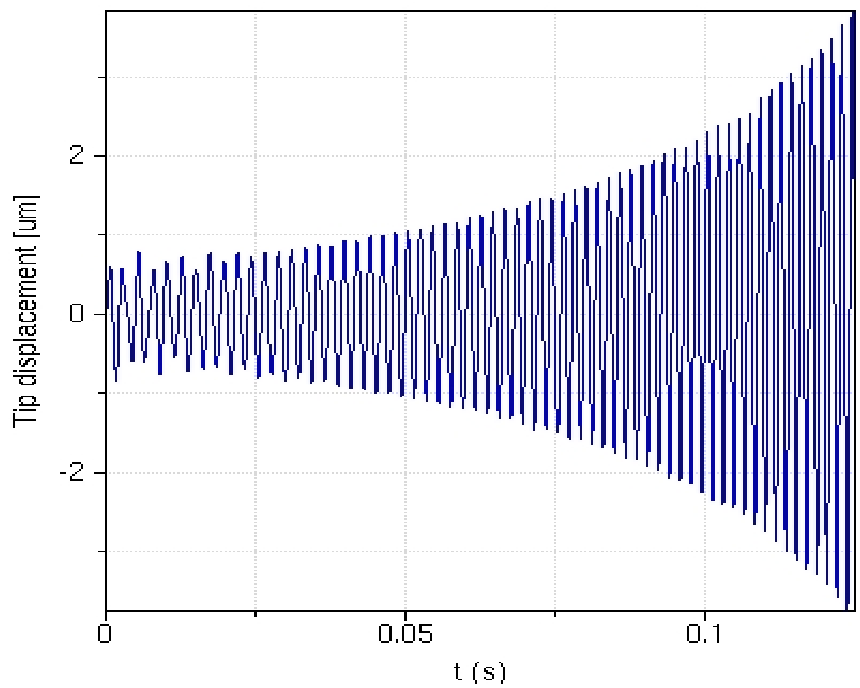

Figure 5.19. Maximum displacement waveform of simulation result

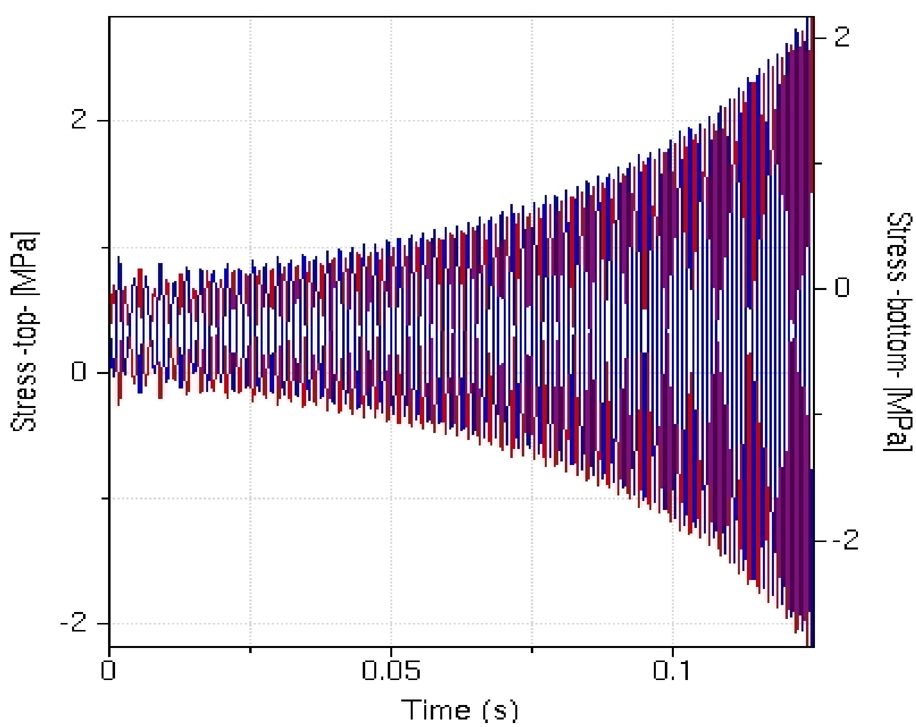

Figure 5.20. Applied stress waveform of simulation result

Table 5.9. Simulation data of serial number 4

S/N	Mass of body (g)	Thickness of PZT (µm)	Thickness of substrate (µm)	Length of substrate (mm)	Excitation / Natural frequency Hz	Open-circuit resonant frequency (Hz)	Average harvested power (µW)	Peak power (µW)	Diode voltage Threshold	Peak Voltage (mV)
4	40	1450	1450	24.53	584.79	613.00	30.37	207.36	0.01	1255.35

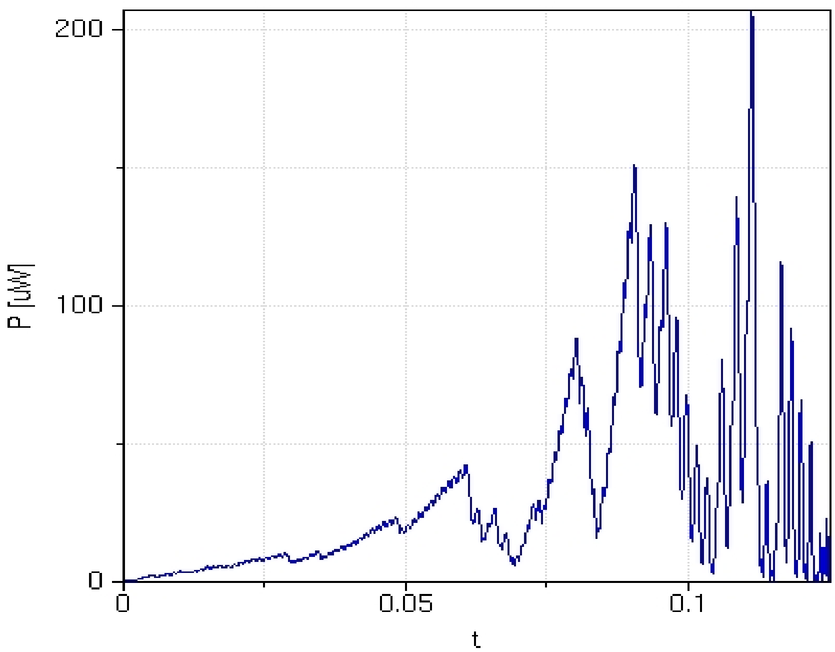

Figure 5.21. Peak output power waveform of simulation result [4]

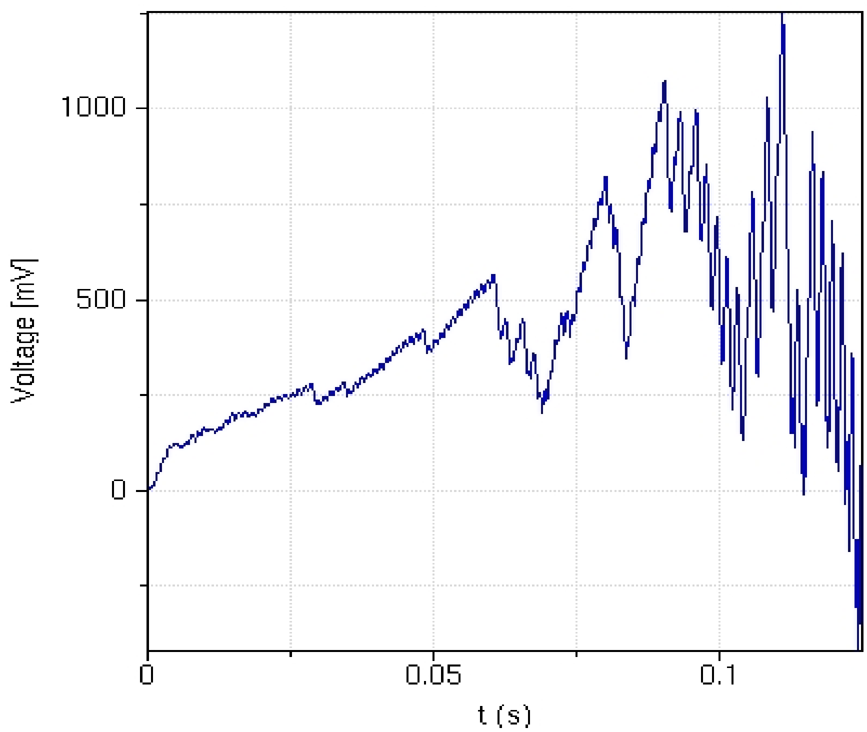

Figure 5.22. Output Voltage Level waveform of simulation result [4]

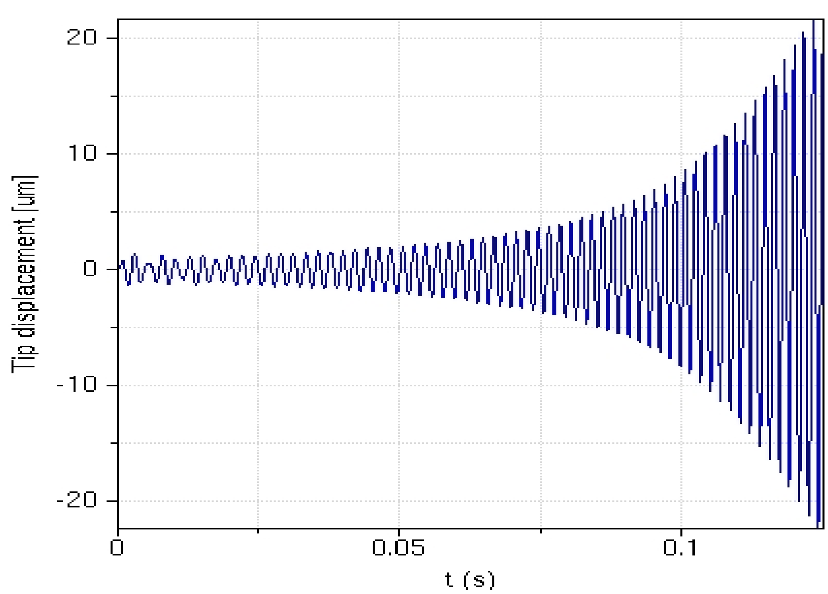

Figure 5.23. Maximum displacement waveform of simulation result

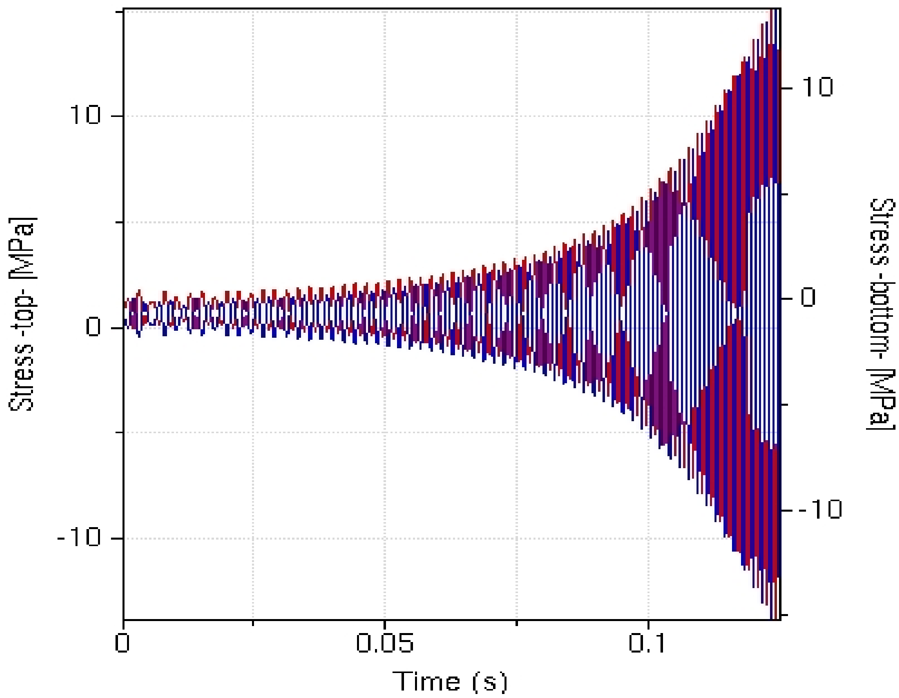

Figure 5.24. Applied stress waveform of simulation result

Table 5.10 Simulation data of serial number 5

S/N	Mass of body (g)	Thickness of PZT (µm)	Thickness of substrate (µm)	Length of substrate (mm)	Excitation/ Natural frequency Hz	Open-circuit resonant frequency (Hz)	Average harvested power (µW)	Peak power (µW)	Diode voltage Threshold	Peak Voltage (mV)
5	50	1450	1450	24.53	524.70	550.00	45.56	597.64	0.01	1987.15

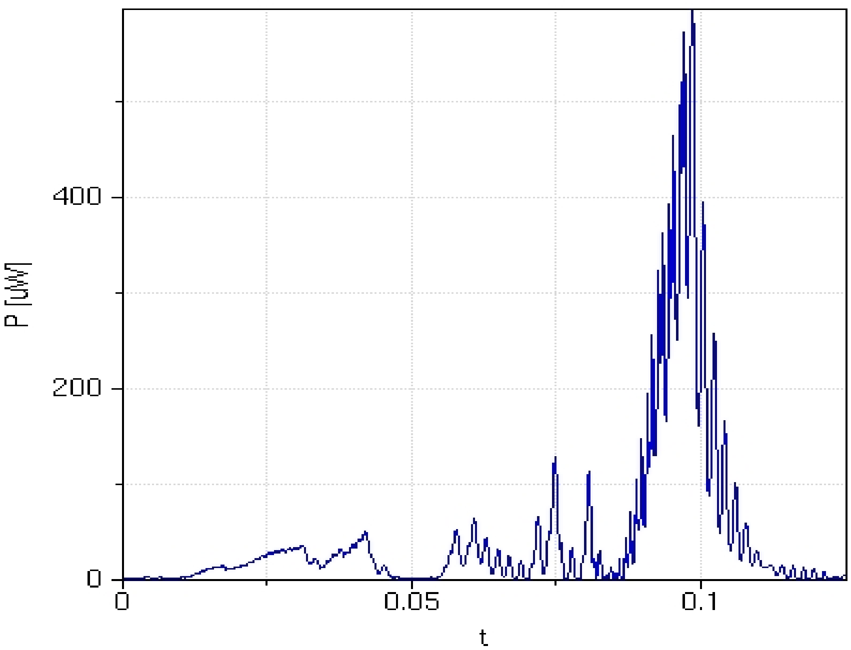

Figure 5.25. Peak output power waveform of simulation result [5]

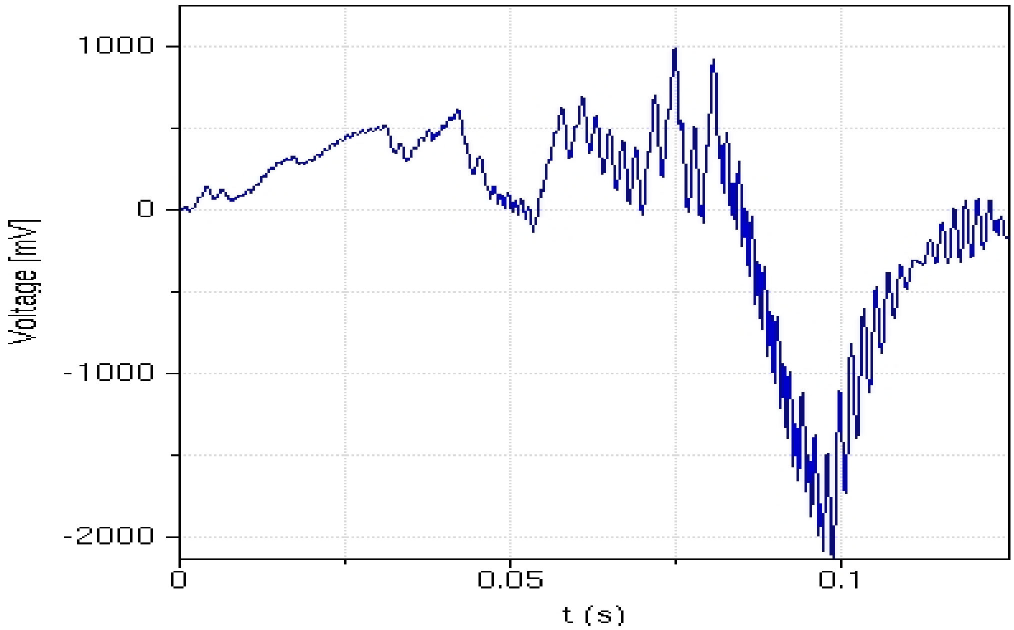

Figure 5.26. Peak output voltage waveform of simulation result [5]

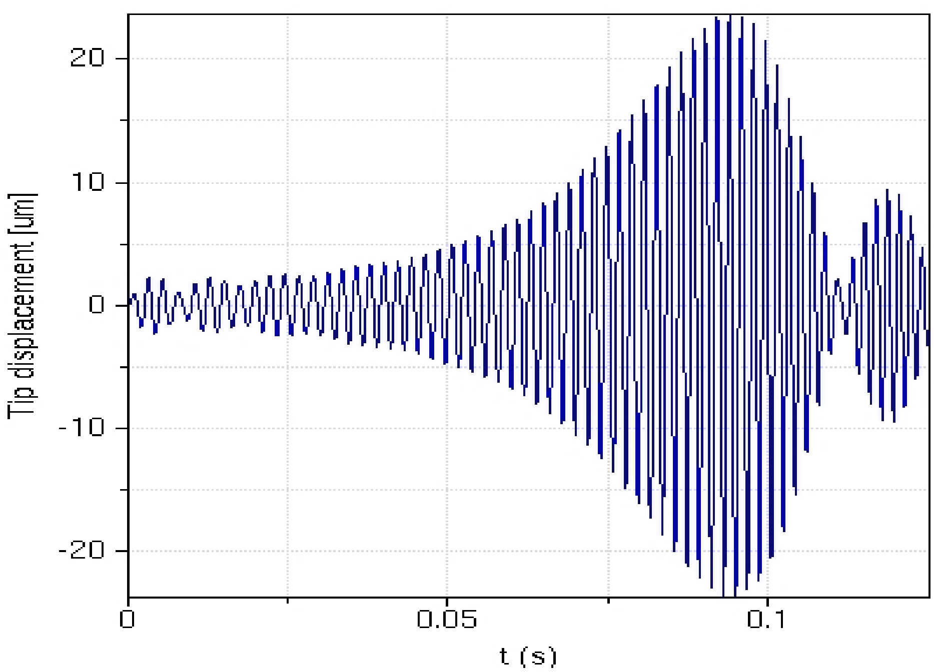

Figure 5.27. Maximum displacement waveform of simulation result [5]

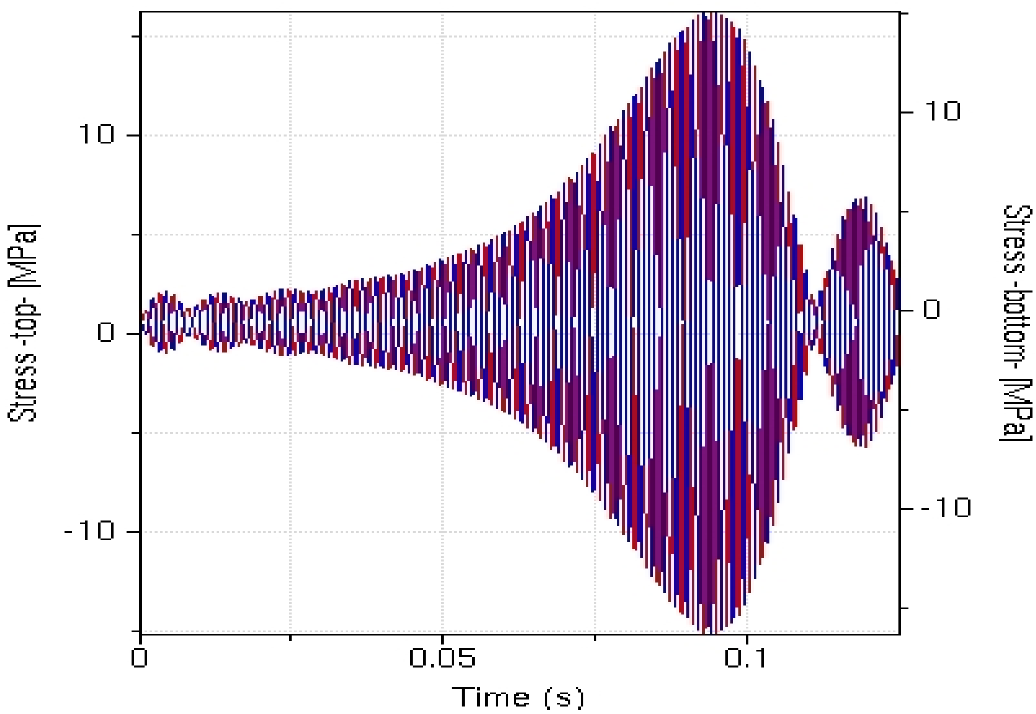

Figure 5.28. Applied stress waveform of simulation result [5]

Table 5.11. Simulation data of serial number 6

S/N	Mass of body (g)	Thickness of PZT (µm)	Thickness of substrate (µm)	Length of substrate (mm)	Excitation/ Natural frequency Hz	Open-circuit resonant frequency (Hz)	Average harvested power (µW)	Peak power (µW)	Diode voltage Threshold	Peak Voltage (mV)
6	60	1450	1450	24.53	479.99	503.14	223.06	2246.00	0.01	4131.54

The table shown above represents the data obtained by tuning the thickness of the PZT energy harvester and the cantilever substrate, to obtain different peak power output and output voltage level when the frequency difference between the natural frequency and open circuit resonant frequency becomes equal 23.9 Hz where the electric field intensity between the dipole of the PZT atomic crystalline structure becomes very strong and the orientation of movement of dipole are shifted from random movement to attain strong polarization and acquire strong and significant piezoelectricity effect.

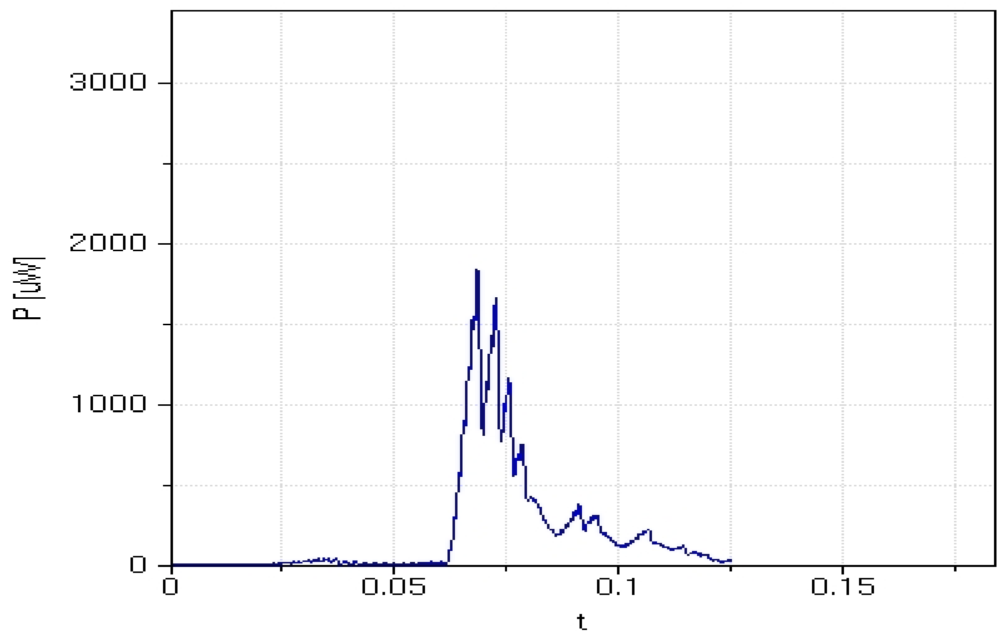

Figure 5.29. Peak output power waveform of simulation result [6]

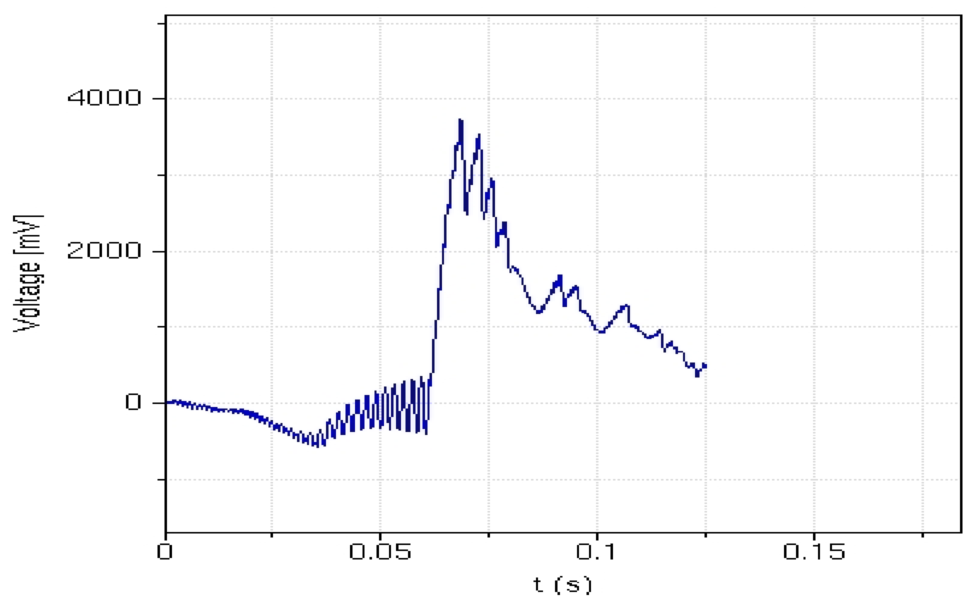

Figure 5.30. Peak output voltage waveform of simulation result [6]

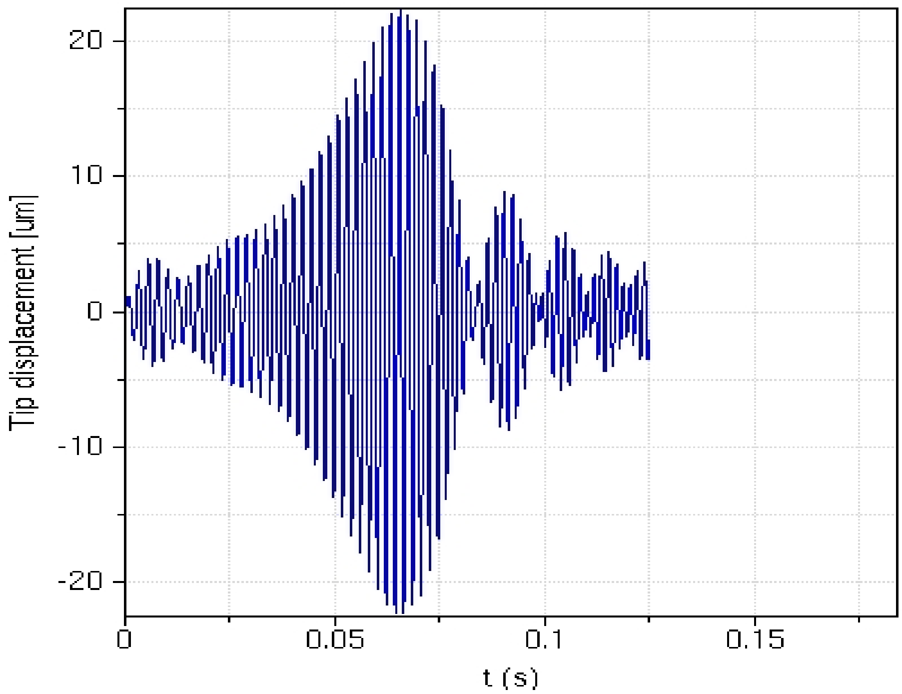

Figure 5.31. Maximum displacement waveform of simulation result [6]

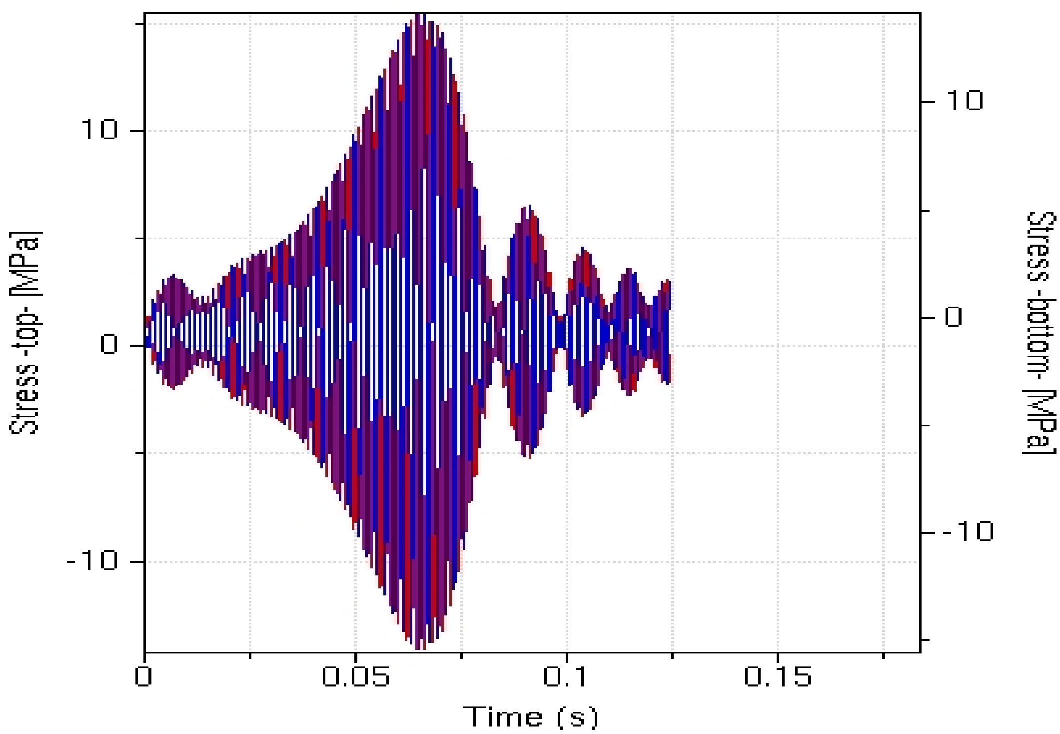

Figure 5.32. Applied stress waveform of simulation result [6]

Table 5.12. Simulation data of serial number 7

S/N	Mass of body (g)	Thickness of PZT (μm)	Thickness of substrate (μm)	Length of substrate (mm)	Excitation/ Natural frequency Hz	Open-circuit resonant frequency (Hz)	Average harvested power (μW)	Peak power (μW)	Diode voltage Threshold	Peak Voltage (mV)
7	56.24	1450	1450	24.53	495.43	519.32	377.38	3451.55	0.01	5121.00

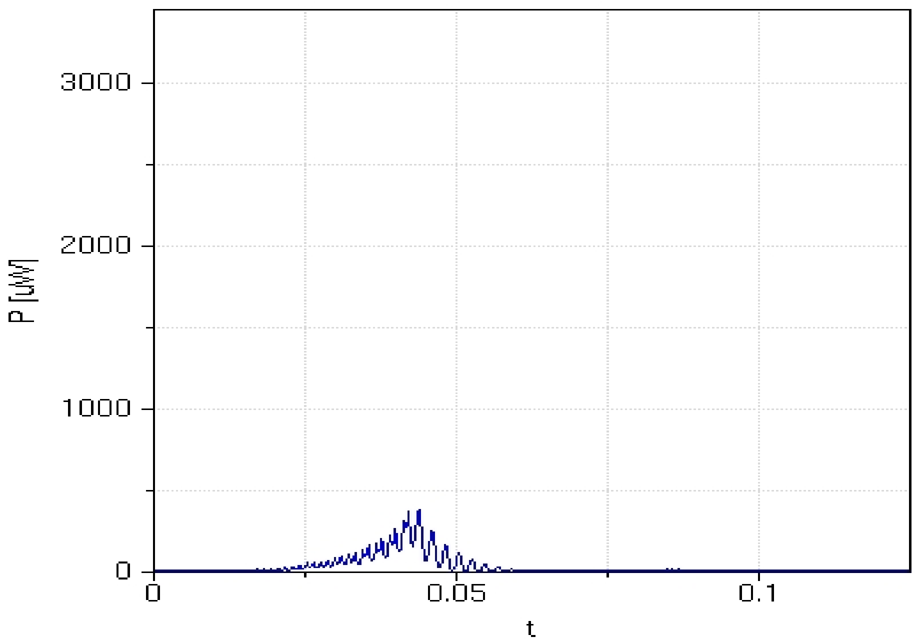

Figure 5.33. Peak output power waveform of simulation result [7]

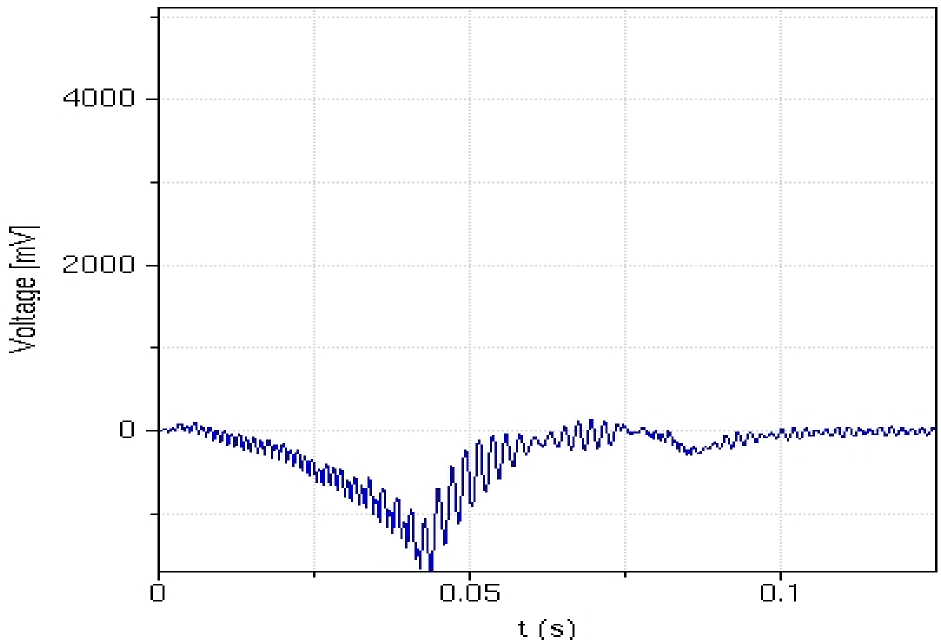

Figure 5.34. Peak output voltage waveform of simulation result [7]

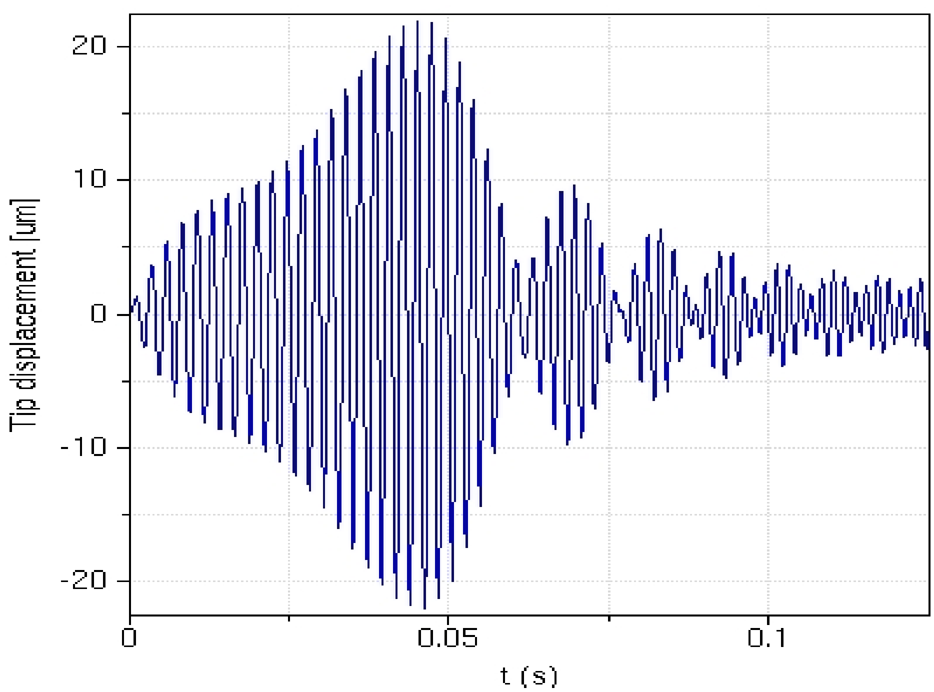

Figure 5.35. Maximum displacement waveform of simulation result [7]

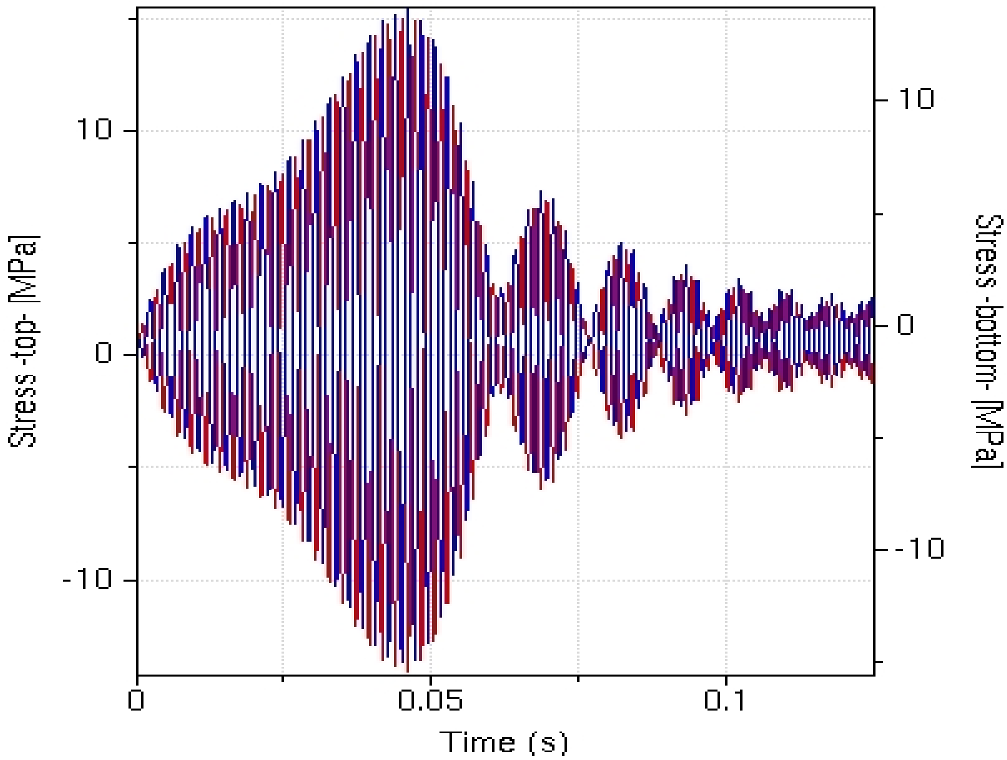

Figure 5.36. Applied stress waveform of simulation result [7]

Table 5.13. thesis data for simulation work

Category B

S/N	Mass of body (g)	Thickness of PZT (µm)	Thickness of substrate (µm)	Length of substrate (mm)	Excitation/ Natural frequency Hz	Open-circuit resonant frequency (Hz)	Average harvested power (µW)	Peak power (µW)	Diode voltage Threshold	Peak Voltage (mV)
8	60	1450	256	24.53	272.24	284.47	0.12	0.00	0.01	0.00

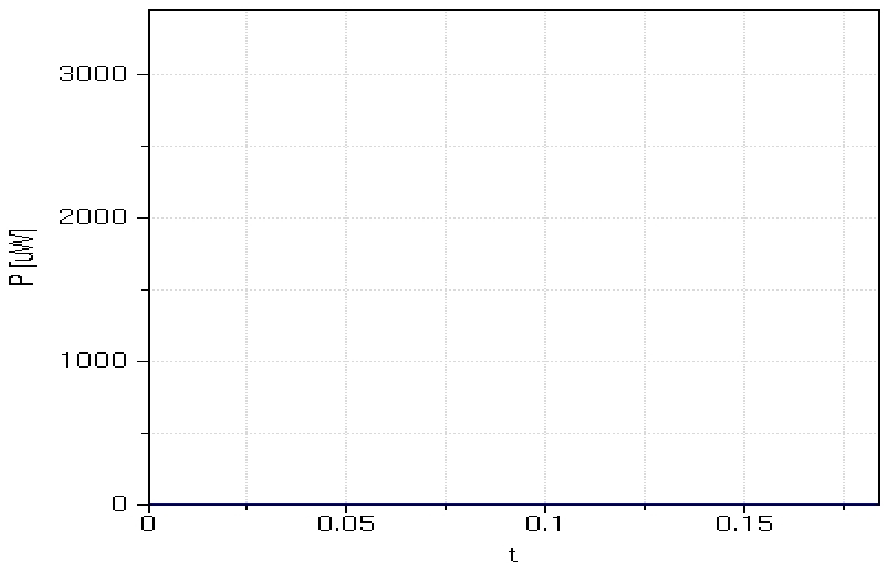

Figure 5.37. Peak power output waveform of simulation result [8]

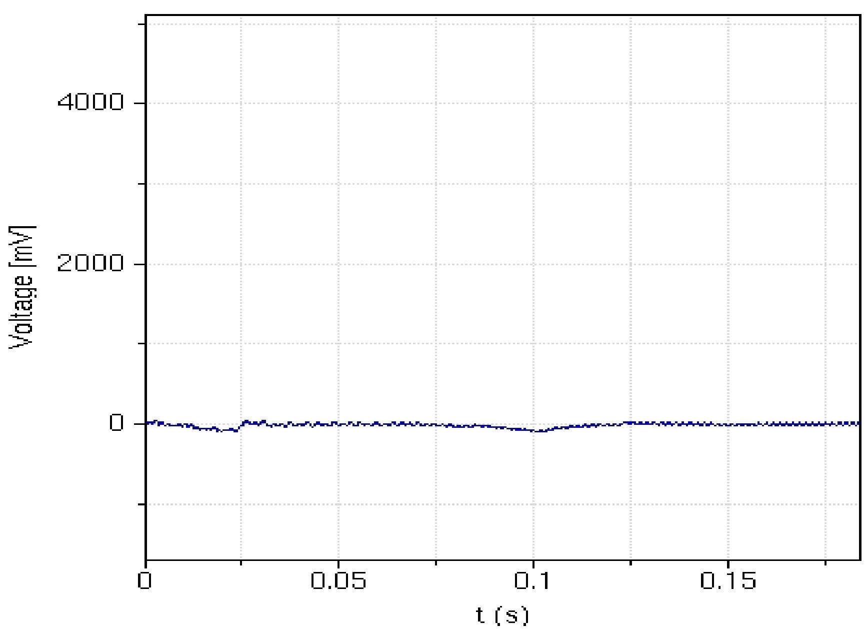

Figure 5.38. Peak output voltage waveform of simulation result [8]

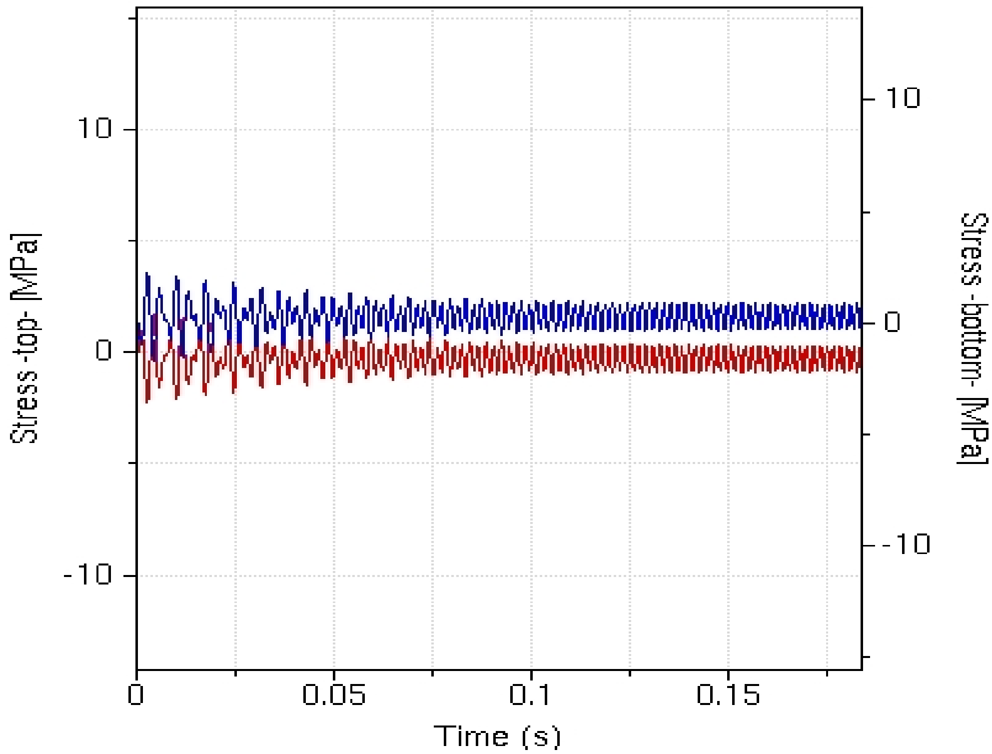

Figure 5.39. Maximum displacement waveform of simulation result [8]

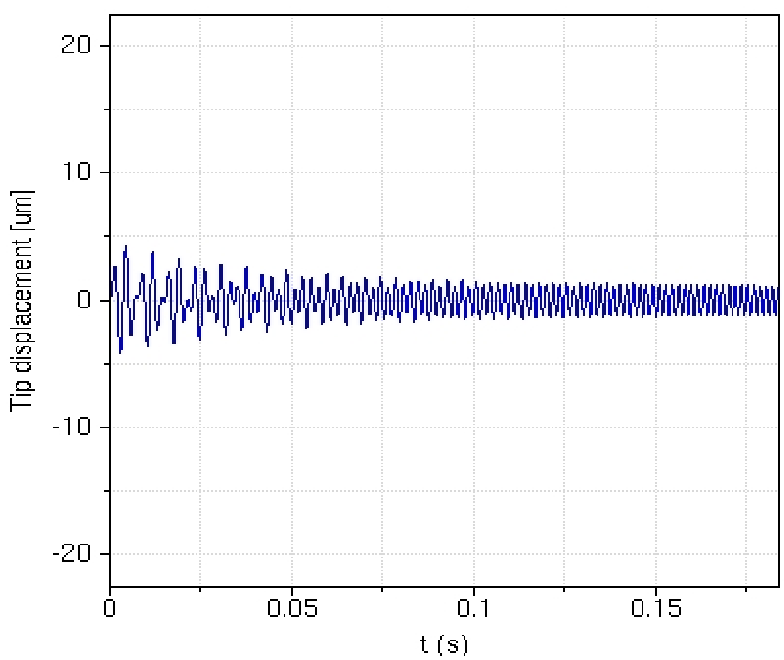

Figure 5.40. Applied stress waveform of simulation result [8]

CHAPTER 6

DISCUSSION

The output voltage measured can be stepped up with the aid of dc-dc converter circuit, however, higher output is possible to be obtained by increasing the thickness of the PZT and thickness and the substrate simultaneously, such that the thickness of the two devices assume equal or almost equal. But maximum output voltage is expected at the same thickness level as demonstrated from the result obtained above.

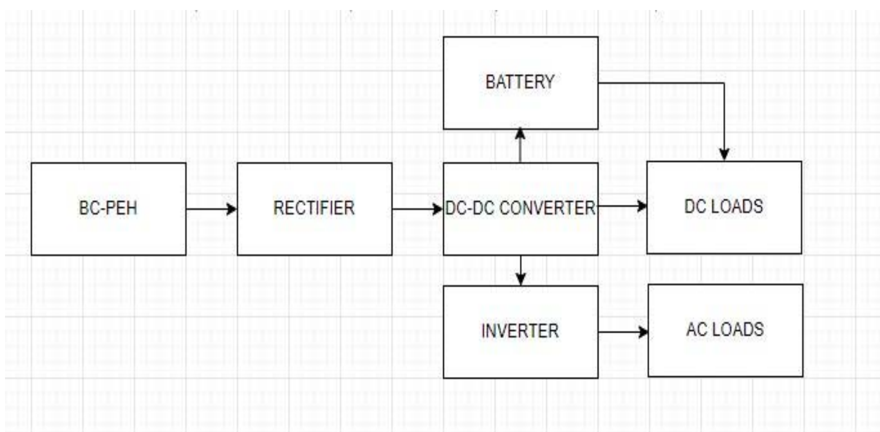

Figure 6.1 Schematic integrated diagram of BC-PEH and DC-DC Converter

The maximum output voltage (5 V) obtained in the experiment 23 above is fed into the DC-DC converter for voltage amplification.

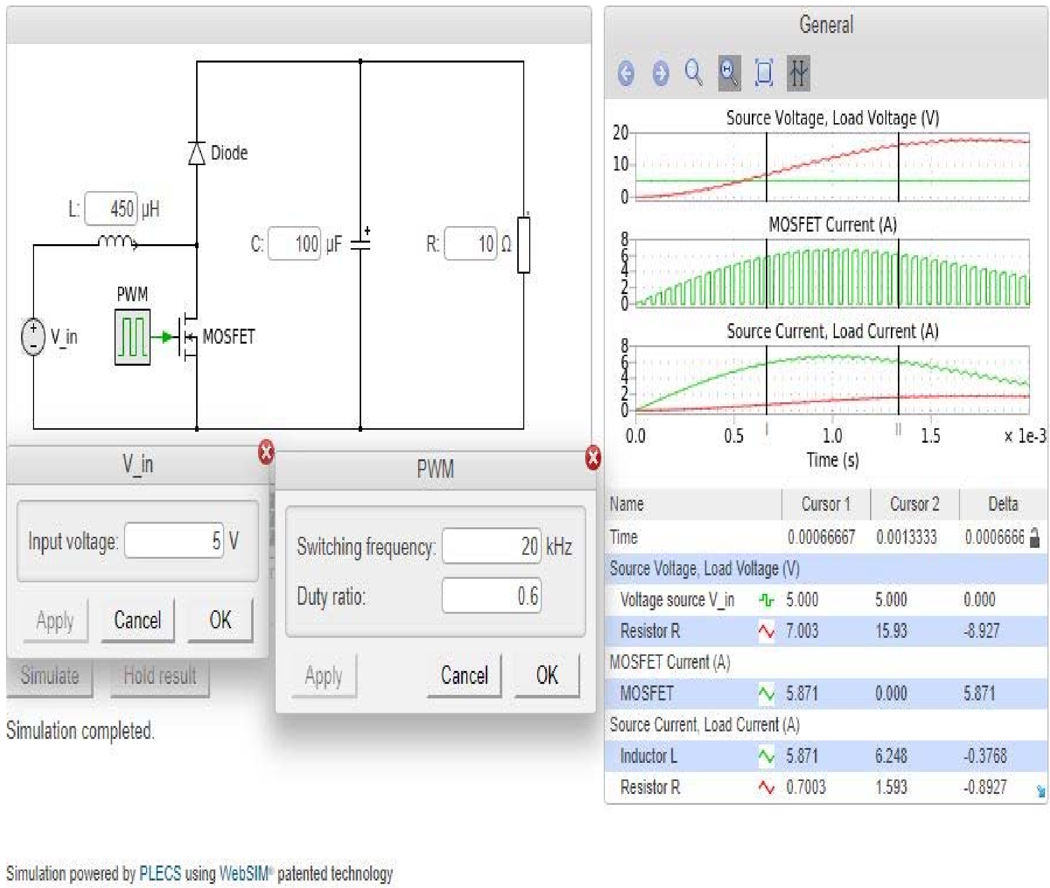

Figure 6.2 PLECS online simulation result of BC-PEH and DC-DC Converter

The output of the piezoelectric harvester is fed into the Boost converter for voltage amplification, however, 5 V input is stepped up to 15 V for charging the 12 V-battery, 12 V- inverter, dc motor and, another DC loads.

6.1.1 Cost Analysis of PZT

The cost description of PZT-5H of various sizes is given as shown below, the type of the PZT used in this thesis work is PZT-5H. according to the simulation, the displayed result is in chapter **5**. Tables 4 and 4d, the test result no15 with waveform figures, 29, 30, 31 and 31

In the simulation result waveform figures, the peak power out and peak output voltage measured were obtained. However, 1450 μm of PZT was applied for the above peak voltage, and peak power among all simulations was achieved.

Table 6.1. cost analysis

Quantity	0.46mm, PZT-5H	0.51mm Square PZT	D75mmSR 40.5mm PZT 8 Material Piezoelectric Ceramics 250khz	22mm 7MHZ PZT Piezo Ceramic for HIFU	20mm 4MHz PZT 8 Transducer	Piezo Ceramics PZT Generator
20-499	$50	$50	-		$30	-
500-999	$30	$30	-		$25	-
1000-4999	$25	$25	-		$22	-
10-99	-	-	$200		-	-
100-999	-	-	$180		-	-
>1000	-	-	$150		-	-
10-499	-	-	-	$30	-	-
500-999	-	-	-	$25	-	-
1000-4999	-	-	-	$22	-	-
>5000	-	-	-	$18	$18	-
10—999						$10
>5000						$8

The worth of the size of PZT material used in the thesis simulation work is less than $50 per 1450 μm according to the price list in the table shown above.

6.1.2 Proposed Engineering and Scientific Solution of PEH

Application of Piezoelectric Sensors is found in soil property determination and in other field of applications. In geotechnical engineering, bender elements are used to determine Gmax of soils by measuring wave velocity through porous media. Compared with a resonant column test, this test offers direct measurements and simpler computations.

In addition to bender testing, resonant column, triaxial and odometer testing can be conducted with the bender element.

Piezoelectric sensor arrays for Gas Leakage Location Based on Correlation of the Time-Space Domain of Continuous Ultrasound. An array of piezoelectric acoustic emission (AE) sensors acquires the propagated signal on the plate's skin. Time continuous signals are generated by gas leakage holes (with diameters under 2 mm). The correlation of signals in the time-space domain can be achieved by collecting and analyzing signals from different sensor positions in the array. Once the sensor array and leakage source are determined, the directional relationship between them can be determined.

A PZT-based guided waves were used for multiple crack detection of steel pipelines and plastic pipe and plastic materials in plastic industries, the detection of preliminary damage has been studied using nonlinear ultrasonic behavior such as higher harmonic generation, subharmonic generation, nonlinear resonance, or mixed frequency response.

6.1.3 Observations

According to the concept of this thesis as discussed in the introductory pages of this paper. Observation of performance output of Piezoelectric output performance will be detailed as follows. Following the series of simulation work conducted for predictions of the output performance of a cantilever energy harvester system.

Since the energy output of a cantilever based-piezoelectric material depends on the factors listed on page 15. However, these are the fundamental factors that dictate the performance of PZT.

Simulation works are categorized into two, Category A depicts the effect of attached mass which describes the input acceleration of the system.

Increasing the attached mass at the free end of cantilever beams but with special consideration of the entire thickness of the piezoelectric material usually increases the expected energy output of the system. At 10 g, 20 g, 30 g 40 g 50 g, peak output voltage increases, from 103.25 mV, 326.98 mV, 675.96 mV, 1255.35 mV, and 1987.15 mV respectively. The corresponding increase in the attached mass of a body and peak output recorded, reduces the frequency band between the natural frequencies and the open-circuit resonant frequencies from 54 Hz, 39.3 Hz, 32.4 Hz, 28.3 Hz, 25.3 Hz respectively.

However, the peak output voltage of 5 V obtained at the lowest different frequency band between natural frequency and open circuit resonant frequency at 23.9 Hz as shown in the table 5.9 and figures 5.9.1.1, 5.9.1.2, 5.9.13, and figure 5.9.1.4 respectively.

According to the CATEGORY B simulation result shown above in **Table 5.3**, it clearly demonstrates the significant effect of shape, size, and volume of Piezoelectric material and the metal substrate on the performance of the system in terms of peak power and peak output voltage of the system.
As the thickness of the metal substrate increases from 256 µm, 512 µm, 768 µm, 1024 µm and 1450 µm while the thickness of the PZT is made constant at 1450 µm. There is similar frequency response. The frequency band difference between the natural frequency and open-circuit resonant frequency increases from 12.2 Hz, 14.4 Hz, 17 Hz, 18.4 Hz and the peak power output and peak output voltage are also observed and recorded at 23.2 Hz when the thickness of PZT and the thickness of the metal substrate assumes equal at 1450 µm respectively.

The system adjustment set up a natural frequency that is nearly close to the resonant frequency of the system. The percentage difference of the calculated frequency is observed to have occurred at a 4% proximity between the natural frequency and the resonant frequency. Hence the peak power output is obtained and recorded.
It was observed that the natural frequency of the system only depends on the following:

- thickness of the PZT
- thickness of the substrate
- the mass of the attached body.

From equation (8) derived above $\omega_n = \sqrt{\frac{k_s}{m}}$

The natural frequency of the system depends on the material stiffness which is a function of the thickness of the PZT and the cantilever beam substrate.

CHAPTER 7

CONCLUSION

In conclusion, according to a series of simulation exercises done and different output voltages and peak power are measured. It is established that in BC-PEH experiment result conducted according to table 5.8, page 71, and 72 in chapter 5 describes that PZT of 1450 μm at the same thickness of the Cantilever substrate delivered the maximum output voltage of 5 V, at almost 5% difference between the excitation frequency and the resonant frequency by increasing the attached mass of a body at its free end from 10 g to 56.24 g where the maximum output voltage is obtained, measured, and recorded.
The maximum output voltage and peak power are obtained when the thickness of the PZT and Cantilever substrate assumes equal or almost equal with increasing the mass of the body attached at its free end.

From the result obtained, there is the flexibility of obtaining a higher output voltage by increasing the thickness of the substrate and PZT along with the mass of the body and this makes this study or technology feasible for microgrid energy solutions as well as renewable energy systems. In addition, the output voltage can be further stepped up with a dc-dc converter to increase the level of the output voltage depending on the desired output level requirement.

As shown above, in page 58, 5 V output from PEH is stepped up to 15 V, therefore, the achieved output depicts the possibility of the proposed solution in this thesis and has the potential to form a fundament solution in gas leakages in LNP plant, pipeline, water system and detection of leakages in plastic industries and other related industries where leakage test is required to pass the quality test in production industries as well as operating micro-scale electronic devices, Internet of Things (IoT), military heel strike shoes, and charging smartphones and tablets.

REFERENCES

[1] Zhou, G., Huang, L., Li, W., & Zhu, Z. (2014). Harvesting ambient environmental energy for wireless sensor networks: a survey. Journal of Sensors, 2014. https://doi.org/10.1155/2014/815467

[2] Chen, W., Cao, Y., & Xie, J. (2015). Piezoelectric and electromagnetic hybrid energy harvester for powering wireless sensor nodes in smart grid. Journal of Mechanical Science and Technology, 29(10), 4313-4318. https://doi.org/10.1007/s12206-015-0928-x

[3] Xiong, Y., Song, F., & Leng, X. (2020). A piezoelectric cantilever-beam energy harvester (PCEH) with a rectangular hole in the metal substrate. Microsystem Technologies, 26(3), 801-810. https://doi.org/10.1007/s00542-019-04608-8

[4] Li, Z., Xin, C., Peng, Y., Wang, M., Luo, J., Xie, S., & Pu, H. (2021). Power Density Improvement of Piezoelectric Energy Harvesters via a Novel Hybridization Scheme with Electromagnetic Transduction. Micromachines, 12(7), 803. https://doi.org/10.3390/mi12070803

[5] Shan, X., Xu, Z., Song, R., & Xie, T. (2013). A new mathematical model for a piezoelectric-electromagnetic hybrid energy harvester. Ferroelectrics, 450(1), 57-65. DOI: 10.1080/00150193.2013.838490

[6] Asthana, P., & Khanna, G. (2019). A broadband piezoelectric energy harvester for IoT based applications. Microelectronics Journal, 93, 104635. https://doi.org/10.1016/j.mejo.2019.104635.

[7] Naano, S. (2019). Research of piezoelectric vibration energy harvesting intended for powering sensors of a pallet lifting and storing system (Doctoral dissertation, Kauno technologijos universitetas).

[8] Shindo, Y., Narita, F., Horiguchi, K., Magara, Y., & Yoshida, M. (2003). Electric fracture and polarization switching properties of piezoelectric ceramic PZT studied by the modified small punch test. Acta materialia, 51(16), 4773-4782.

[9] Wu, Y., Qiu, J., Zhou, S., Ji, H., Chen, Y., & Li, S. (2018). A piezoelectric spring pendulum oscillator used for multi-directional and ultra-low frequency vibration energy harvesting. Applied energy, 231, 600-614.[9].

[10] Asthana, P., & Khanna, G. (2020). Power amplification interface circuit for broadband piezoelectric energy harvester. Microelectronics Journal, 98, 104734.

[11] The Journal of the Acoustical Society of America 70, 1561 (1981); https://doi.org/10.1121/1.387221

[12] Anisi, M.H., Abdul-Salaam, G., Idris, M.Y.I. et al. Energy harvesting and battery power based routing in wireless sensor networks. Wireless Netw 23, 249–266 (2017). https://doi.org/10.1007/s11276-015-1150-6

[13] Kohei Maruyama, Yoshihiro Kawakami, Kotaro Mori, Hiroki Kurita, Yu Shi, Yu Jia, Fumio Narita, Electromechanical characterization and kinetic energy harvesting of piezoelectric nanocomposites reinforced with glass fibers, Composites Science and Technology,Volume223,2022,109408,ISSN02663538, https://doi.org/10.1016/j.compscitech.2022.109408

[14] Yu, Y., & Narita, F. (2021). Evaluation of Electromechanical Properties and Conversion Efficiency of Piezoelectric Nanocomposites with Carbon-Fiber-Reinforced Polymer Electrodes for Stress Sensing and Energy Harvesting. *Polymers*, *13*(18), 3184. MDPI AG. Retrieved from http://dx.doi.org/10.3390/polym13183184

[15] Dhote, S. (2016). Design and development of broadband piezoelectric vibration energy harvester based on compliant orthoplanar spring (Order No. 10194382). Available from ProQuest Dissertations & Theses Global. (1884574028). Retrieved from: https://www.proquest.com/dissertations-theses/design-development-broadband-piezoelectric/docview/1884574028/se-2

[16] Datta, S. (2014). Piezoelectric Materials: Crystal Orientation and Poling Direction. Retrieved from: https://www.comsol.com/blogs/piezoelectric-materials-crystal-orientation-poling-direction/. (Acessed July, 2022).

[17] Henan Song, Xiaobiao Shan, Lanshuang Zhang et al., "Research on identification and active vibration control of cantilever structure based on NARX neural network", Mechanical Systems and Signal Processing 171, pg. 108872, (2022); doi:10.1016/j.ymssp.2022.108872

[18] Seyyed Masoud Kargar, Guangbo Hao, "An Atlas of Piezoelectric Energy Harvesters in Oceanic Applications", Sensors 22(5), pg. 1949, (2022); doi:10.3390/s22051949

[19] J.C. Park, D. H. Lee, J. Y. Park, Y. S. Chang and Y. P. Lee, "High performance piezoelectric MEMS energy harvester based on $D33$ mode of PZT thin film on buffer-layer with $PbTiO3$ inter-layer," IEEE Solid- State Sensors, Actuators and Microsystems Conference, pp. 517 – 520,June 2009.

[20] P. Muralta, M. Marzenckib, B. Belgacema, F. Calamea and S. Basrourb, "Vibration energy harvesting with PZT micro device," Elsevier Proceedings of the Eurosensors XXIII conference, pp. 1194–1196, 2009.

[21] R. G. Bryant, R. T. Effinger, I. Aranda, B. M. Copeland, E. W. Covington, and J. M. Hogge, J. Intell. Mater. Syst. Struct. 15(7), 527–538 (2004).

[22] R. G. Bryant, NASA Technical Report 20080000875, 2007.

[23] Z. Chen, Y. Hu, and J. Yang, Appl. Math. Mech. 28(6), 779–784 (2007).

[24] A. Massaro, S. De Guido, I. Ingrosso, R. Cingolani, M. De Vittorio, M. Cori, A. Bertacchini, L. Larcher, and A. Passaseo, Appl. Phys. Lett. 98(5), 053502 (2011).

[25] H. Liu, C. Lee, T. Kobayashi, C. Tay, and C. Quan, Microsyst. Technol. 18(4), 497–506 (2012).

[26] H. Liu, C. Lee, T. Kobayashi, C. Tay, and C. Quan, Sens. Actuators, A 186, 242–248 (2012).

[27] Y. Qi and M. C. McAlpine, Energy Environ. Sci. 3(9), 1275–1285(2010).

[28] C. Dagdeviren, B. Yang, Y. Su, P. L. Tran, P. Joe, E. Anderson, J. Xia, V. Doraiswamy, B. Dehdashti, X. Feng, B. Lu, R. Poston, Z. Khalpey, R. Ghaffari, Y. Huang, M. J. Slepian, and J. A. Rogers, Proc. Natl. Acad. Sci. 111, 1927 (2014).

[29] Z. L. Wang and J. Song, Science 312(5771), 242–246 (2006).

[30] G. Zhu, R. Yang, S. Wang, and Z. Wang, Nano Lett. 10(8), 3151–3155 (2010).

[31] Sensor Technology Limited, see http://www.sensortech.ca/site/index.cfm?DSP=Page&ID=125 for properties of the BM532 lead zirconate titanate (last accessed October 1, 2014).

[32] Channel Technologies Group, see http://www.channeltechgroup.com/publication/view/pmn-32pt-001/ for properties of PMN-32PT single crystal (last accessed October 1, 2014).

[33] T. R. Gururaja, W. A. Schulze, L. E. Cross, R. E. Newnham, B. A. Auld, and Y. J. Wang, IEEE Trans. Sonics Ultrason. 32(4), 481–498 (1985).

[34] L. F. Brown, IEEE Ultrason. Symp. 1–2, 539–550 (1992).

[35] W. A. Smith, “New Opportunities in Ultrasonic Transducers Emerging from Innovations in Piezoelectric Materials,” Proc. SPIE 1733, 3–26 (1992).

[36] R. A. Islam and S. Priya, Appl. Phys. Lett. 88(3), 032903 (2006).

[37] C. H. Choi, I. T. Seo, D. Song, M. S. Jang, B. Y. Kim, S. Nahm, T. H. Sung, and H. C. Song, J. Eur. Ceram. Soc. 33(7), 1343–1347 (2013).

[38] K. Miso, H. Mathias, D. John, and L. W. Brian, Smart Mater. Struct. 19(4), 045023 (2010).

[39] H. A. Sodano, G. Park, D. J. Leo, and D. J. Inman, Proc. SPIE 5050, 101–108 (2003).

[40] J. Yuan, T. Xie, and W. Chen, IEEE Ultrason. Symp. 1–4, 1397–1440 (2008).

[41] S. R. Platt, S. Farritor, K. Garvin, and H. Haider, IEEE/ASME Trans. Mechatron. 10(4), 455–461 (2005).

[42] M. Renaud, P. Fiorini, R. van Schaijk, and C. van Hoof, Smart Mater. Struct. 18(3), 035001 (2009).

[43] J. S. Harrison and Z. Ounaies, NASA/CR-2001-211422, ICASE Report 2001-43, 2001.

[44] C. J. Kendall, BS thesis, Massachusetts Institute of Technology, 1998.

[45] H. A. Sodano, J. Granstrom, J. Feenstra, and K. Farinholt, Proc. SPIE 6525, 652502 (2007).

[46] N. Elvin, A. Elvin, and D. H. Choi, J. Strain Anal. Eng. Des. 38(2), 115–124 (2003).

[47] S. Pobering and N. Schwesinger, in Proceedings of the International Conference on Mems, Nano and Smart Systems (IEEE, 2004), p. 480.

[48] D. Vatansever, R. L. Hadimani, T. Shah, and E. Siores, Smart Mater. Struct. 20(5), 055019 (2011).

[49] S. Li, J. Yuan, and H. Lipson, J. Appl. Phys. 109(2), 026104 (2011).

[50] S. J. Oh, H. J. Han, S. B. Han, J. Y. Lee, and W. G. Chun, Int. J. Energy Res. 34(5), 431–437 (2010).